Use of Supercritical Propylene to Produce Polypropylene/Clay Nanocomposites via *in situ* Polymerization

by

Manoel Lisboa da Silva Neto

A thesis

presented to the University of Waterloo

in fulfillment of the

thesis requirement for the degree of

Master of Applied Science

in

Chemical Engineering

Waterloo, Ontario, Canada, 2014

AUTHOR'S DECLARATION

I hereby declare that I am the sole author of this thesis. This is a true copy of the thesis, including any required final revisions, as accepted by my examiners.

I understand that my thesis may be made electronically available to the public.

ABSTRACT

Nanocomposites have been receiving a lot the attention in the last decade from both industry and academia, since a small amount of nanofiller can significantly improve the materials properties. In the field of thermoplastics, polypropylene (PP) is one of the most used materials , due its easy processability, good balance of mechanical properties, and low cost. However, PP has certain shortcomings such as poor gas barrier and low thermal stability which limit its application. In order to be classified as nanocomposite the material needs to have at least one phase with one dimension less than 100nm. The properties achieved by nanocomposites will depend on the type of polymer, type of dispersed phase (filler), surface interaction between filler and polymer, and the production method. Nanofillers present many shapes and sizes, but they can be grouped in nanoparticles, nanotubes and nanoplates.

Montmorillonite (MMT) is a clay that has been extensively studied to produce PP nanocomposites, due to its availability, high aspect ratio, high modulus and high cation exchange capacity, characteristics that result in composite with improved properties. Three different morphologies can be observed in PP/MMT nanocomposites: agglomerates (similar to the conventional composites); intercalated; or exfoliated. Among these morphologies, exfoliation is the most desirable and the hardest to be achieved in PP/MMT nanocomposites.

Several methods have been used to produce PP nanocomposites. They can be grouped in three main groups: solution blending; melt processing; and *in situ* polymerization. In order to produce an exfoliated nanocomposite, some methods have assisted the exfoliation using supercritical fluids. Supercritical carbon dioxide is by far the most explored one.

Polypropylene is a semi-crystalline polymer and its properties rely on amount of its crystallinity, which is related to its stereochemical configurations. Isotactic PP and syndiotactic PP result in a semi-crystalline polymer while atactic results in an amorphous polymer. Two catalyst systems can be used to produce isotactic PP: Metallocene and Ziegler-Natta (ZN).

This research study was carried out in order to develop an appropriated process to produce PP/MMT nanocomposites with a high level of exfoliation using in situ polymerization assisted by supercritical propylene. The main idea is to use supercritical propylene to treat the montmorillonite before polymerization. In this process, the small

molecules of propylene diffuse inside the clay galleries under supercritical conditions (high pressure and temperature) until reaching complete saturation. Once this saturation is reached the mixture of polypropylene and clay is catastrophically decompressed and fed into an autoclave reactor. The propylene polymerization reaction is them catalyzed by ZN catalyst. The pressure of the mixture of propylene-montmorillonite from the supercritical condition to the reactor autoclave decreased significantly, allowing propylene to expand and exfoliate the clay as it was fed in the reactor. Propylene in supercritical conditions was used in this works because it is the monomer for the subsequently polymerization and because its good properties at supercritical conditions.

In order to evaluate the results the following methods were used: transmission electron microscopy (TEM) to investigate the nanoscale sample morphology and evaluate the clay exfoliation, X-ray diffraction (XRD) to determine interlamellar distance, d_{001}, of the clay, differential scanning calorimetry (DSC) to determine the amount of crystallization of polymer and composite, thermogravimetric analysis (TGA) to determine composite clay content, scanning electron microscopy (SEM) to evaluate the morphology, and clay swelling test to evaluate the compatibility among various pairs clays-solvent.

The first part of this work evaluated the interaction and swelling effects of different pairs of clay-solvent with or without sonication. This was necessary in order to choose the best clay to carry out the study. Four solvents with different polarity (chlorobenzene, toluene, cyclohexane and hexane) and eight clays (seven organically modified and one unmodified) were evaluated with or without sonication. Closite 15A and 93A presented the best results with different solvents and they were selected for further experiments. The experiments also showed that sonication improves the swelling of the clay.

Initial screening of the polymerization reaction was carried out using two conditions: feeding supercritical propylene without clay and adding clay without the addition of supercritical fluid.

The addition of supercritical propylene did not modify the morphology and properties of PP in comparison to the normal polymerization. The addition of Cloisite 15A or Cloisite 93A (pre-treated with toluene, not with supercritical propylene) produced nanocomposites. Although Cloisite 15A showed better results on the swelling tests, Cloisite 93A presented much better polymerization yield, therefore it was selected for further investigation using treatment with supercritical propylene. Cloisite93A was

submitted to a treatment under four different supercritical propylene conditions (temperature and pressure) for thirty minutes. Each mixture was subsequently fed to the reactor through a catastrophic expansion inside an autoclave reactor running a propylene polymerization reaction. The results from XRD and TEM show a significant improvement on the exfoliation when treating the clay under supercritical propylene conditions followed by in situ polymerization, as compared to the in situ polymerization without treating the clay with supercritical propylene. In conclusion, the utilization of supercritical propylene has improved the dispersion of the clay at the nanoscale during the preparation of these nanocomposites by in situ polymerization.

ACKNOWLEDGEMENTS

DEDICATION

I dedicate this work to my father (in memoriam). He was a man who had a low-level of education, but a lot of wisdom. I thank him for teaching me that hard work, honesty and respect for others are key values to be followed.

TABLE OF CONTENTS

LIST OF FIGURES

XI

LIST OF TABLES

1 INTRODUCTION

1.1 Motivation

Polypropylene (PP) is one of the most widely used thermoplastics in the world due to its combination of easy processability, good balance of mechanical properties and low cost [1]. The extraordinary versatility of different polypropylene grades, including its homopolymers and both copolymers (block and random) are suitable for a wide variety of applications, such as fibers, films, injection and blow molded parts and many others. However, polypropylene has certain shortcomings that limit its use in some applications. One of these limitations is its poor oxygen barrier that prevents the widespread use of this material in the packaging industry. Additionally, its low thermal stability limits further utilization in automotive parts.

Nanotechnology may be used to overcome these limitations because polymer/nanoclay nanocomposites demonstrate improved oxygen barriers and thermal properties [2]. In fact, some nanocomposites of nanoclay and polar matrices are already being used in industrial applications. Probably the most well-known example is polyamide 6 reinforced with montmorillonite (MMT) used in automotive parts by Toyota [2, 4]. Nanocomposites of MMT with different matrices presenting high barrier properties are also commercially available [4].

MMT is a naturally occurring 2:1 phyllosilicate. The MMT structure consists of 1nm thin layers, with a central octahedral sheet of alumina sharing oxygen atoms with two external silica tetrahedral sheets. Isomorphic substitution within the layers generates a negative charge on the layer's surface. This charge is balanced by hydrated cations in the interlayer [5].

Several research groups have dedicated substantial effort toward improving the properties of PP/MMT nanocomposites [6, 9]. However, due to the lack of polar groups in the PP chains, it is still a challenge to disperse nonpolar nanofiller, like MMT, into a PP matrix.

Several methods have been described for the preparation of PP/MMT nanocomposites. Melt compounding is by far the most cited in the literature due to the easy processability of PP and the use of conventional processing equipment [7, 8]. In this method, the MMT is mixed with PP above the melting temperature of the polymer

through the shearing process. Under these conditions, the polymer chains can eventually intercalate in the clay interlayers leading to exfoliation [10, 11].

The solution blending method is based on the swelling capacity of the MMT. In this procedure, the clay swells in a solvent that is also able to dissolve the PP [12]. This three component mixture is prepared with the aid of heat and stirring. After intense mixing, the solvent is removed by evaporation or the polymer is precipitated by the addition of a non-solvent. Although the solution blending method is not suitable for industrial production of polyolefin nanocomposites, it has been studied for fundamental purposes [13, 14].

In situ polymerization is a method that has been receiving increased attention in recent years. This synthetic route avoids the enthalpic and entropic barriers that prohibit the intercalation of non-polar polypropylene chains into the polar MMT interlayers. The first step in preparing PP/MMT nanocomposites by *in situ* polymerization involves supporting the catalyst (Ziegler-Natta or metallocene) into the clay galleries. Next, the supported catalyst is used in the polymerization of propene [15, 16]. The objective of this method is to grow the polymer chains outward from the clay galleries producing exfoliated nanocomposites. Although significant progress has been made in the synthesis of PP/MMT via *in situ* polymerization, a few problems still need to be overcome in order to produce nanocomposites at industrial scales. Among them are poor adhesion between the clay and the polymer matrix, reduced control of the polymer molecular structure, and poor morphology of the polymer particle.

Recently, Dal Castel [17] studied the preparation of PP/MMT nanocomposites using Ziegler-Natta catalyst with controlled morphology using the slurry process Under these conditions, the catalyst retained its characteristics of producing polymer particles with appropriated morphology with good dispersion of the clay. However, donors were not added to the catalyst and the PP obtained presented a low isotactic index.

The use of a supercritical fluid to exfoliate the MMT has been considered as an alternate route for the preparation of polymer/clay nanocomposites with increased dispersion levels and, consequently, improved properties. Supercritical fluids have been used as a solvent to improve the dispersion of MMT in polymeric matrices, such as poly(methyl methacrylate) [18], polystyrene [19], polylactide [20], during *in situ* polymerization. Supercritical fluids have also been used to swell the MMT in solution blending [21] and melt compounding procedures [22, 23].

Manke and coworkers [24] developed a process where the clay is swelled with supercritical carbon dioxide in a pressurized vessel and then catastrophically depressurized to atmospheric pressure so that the stacked clay layers are forced apart. The exfoliation of the clay was identified by x-ray diffraction (XRD) and scanning electron microscopy (SEM). These methods present a promising approach to increase the dispersion of MMT in PP because the clay layers are separated prior to the mixture with the polymer.

1.2 Objectives and Scope

The aim of this work was to carry out a study to further evaluate the method for preparation of polypropylene-clay nanocomposites. The initial part of the study carried out and extensive evaluation of solvent-clay interaction and swelling effects. This initial study was necessary to select a modified-MMT for this study. The modified MMT was submitted to dispersion in supercritical propylene and subsequently to a catastrophic expansion inside an autoclave reactor to produce polypropylene nanocomposites by *in situ* polymerization. The effect of the pressure and temperature on the fluid, near and far above its critical point, on the structure and thermal properties of PP/MMT nanocomposites was investigated. The clay was treated with supercritical propylene which was also the monomer for the polymerization. The *in situ* polymerizations were carried out using a supported Ziegler-Natta catalyst in a slurry process.

1.3 Document Outline

This thesis is organized in five main chapters, as follows:
- Chapter 1 – Introduces the reader to the thesis topic, motivation to conduct the study and gives a brief description of the document.
- Chapter 2 – Presents the literature review on polymer/clay nanocomposites. It includes the preparation methods and relevant properties of polymeric nanocomposites, mainly the PP/MMT nanocomposites. A brief review on the properties of supercritical fluids is also presented.
- Chapter 3 – Describes the materials that were employed in the experimental work; explains the methodology used for preparation of the

PP/MMT nanocomposites; and the techniques and procedures followed to assess some of the final properties of the nanocomposites prepared.

- Chapter 4 – Presents the experimental results and discussions for the preparation and characterization of PP/MMT nanocomposites.

- Chapter 5 – Gives general concluding remarks, along with recommendations for future work.

2 LITERATURE REVIEW

This chapter presents the theoretical background on polymer nanocomposites, especially polypropylene-montmorillonite (PP/MMT). A broad literature review comprising of structure, properties and preparation of these materials is presented.

2.1 Polymer Based Nanocomposites

Conventional composite materials are defined as materials made from two or more materials with significantly different physical or chemical properties which remain separate and distinct within the finished structure. The combination of these materials must exhibit a significant proportion of the properties of both materials, so that a better combination of properties is achieved [25]. The nanocomposites differ from conventional composites by having at least one of their constituent materials with one, two or three dimensions of less than 100 nanometers [2]. One of the main advantages of the nanocomposites is the significant improvement of properties at low nanofiller loadings. Two examples of significant improvement in properties were presented by Sandler *at al* . [26], and Fornes and Paul [27]. Sandler *et al.* [26] added aligned carbon nanotubes in an epoxy matrix and achieved electrical percolation threshold at 0.0025wt%. It is necessary to use at least 400 times more of a conventional filler, such as carbon black, to achieve the same results [28]. Fornes and Paul [27] presented a 100% increase in the modulus of nylon nanocomposites when only 5%wt of MMT was added. A loading of 20%wt is needed to achieve the same effect using glass fiber. Another advantage of the nanocomposites is that the low loading levels have low impact on other properties of the polymer matrix, such as processability and density.

The main difference between the nanofillers and traditional micrometer-scale fillers is obviously the size. This small size can bring intrinsic advantages. For example, smaller particles create lower stress concentrations and consequently do not compromise the ductility of the polymer. Additional advantages are that nanofillers are able to increase mechanical and electrical properties without affecting polymer optical clarity, since very small particles do not cause light scattering. The small size of nanofillers can lead to unique properties of the particles themselves (single-wall carbon nanotubes are the stiffest material known) [29]. In addition, the small size of the fillers leads to an exceptionally large interfacial area in the nanocomposites. The interfacial region can present altered chemical or physical properties, such as chain mobility or

crystallinity, and has been reported to be as small 2nm and as large as 50nm. Even though the interfacial region is only a few nanometers, a great portion of the matrix behaves differently from the pure matrix. For example, if the interfacial region is 10nm around spherical particles with 15nm in diameter, the interfacial region would correspond to practically the whole matrix at 5% loading, as shown in Figure 1 [30].
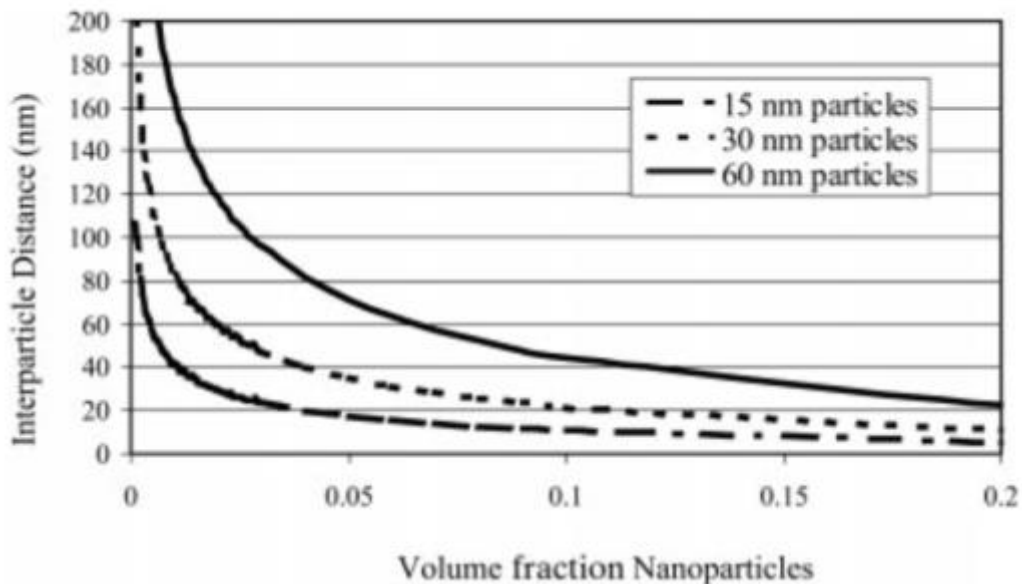
Figure 1. Interparticle spacing as a function of particle size for spherical nanoparticles ideally dispersed in a composite [30].

Nanofillers come in many shapes and sizes. However, they can be grouped into three categories: nanoparticles, nanotubes, and nanoplates, according to the number of dimensions in the nanometer scale [31]. Several nanomaterials have been used as filler to improve different properties of polymeric nanocomposites, such as silica [32], fullerenes [33], metallic oxides [34], nanocellulose [35], carbon nanotubes [36], metallic nanowires [37], natural and synthetic nanoclays [38], and graphite [39].

MMT is by far the most studied nanofiller for the production of PP nanocomposites due to its availability (vast natural deposits around the globe) [40], high aspect ratio (50-200), high modulus (178 GPa) [27] and high cation exchange capacity (80-150mEq/100g) [41].

2.2 Montmorillonite (MMT)

MMT belongs to the general family of 2:1 layered silicates with a general formula $(Al, Mg, Fe)_4(Si, Al)_8O_{20}(OH)_4(1/2Ca, Na)_{0,7}.nH_2O$ [42]. Its crystal structure consist of layers made up of 2 silica tetrahedral sheets sandwiching a central octahedral sheet of aluminum oxide, as show in Figure 2. The stacking of these layers leads to a gap between the layers called the interlamellar gallery (d_{001}). Typical Van der Waals forces are active in this domain. Isomorphic substitution of Si^{4+} atoms by Al^{3+} in the tetrahedral positions and Al^{3+} atoms by Mg^{2+} or Fe^{2+} in the octahedral positions generates negative charges that are normally counterbalanced by cations residing in the interlayer space. These cations are usually hydrated Na^+, K^+, or Ca^{+2} in naturally occurring MMT. This structure is highly hydrophilic, and it is not miscible with most polymers, including PP. Ion exchange reactions of interlayer cations with organic cations, such as phosphonium [43], imidazolium [19] and more often alkylammonium salts [44], are used to reduce the hydrophilic character of the clay. These organic salts can add functional groups that can react with the polymer matrix, or in some cases initiate the polymerization of monomers to improve the strength of the interface between the inorganic and the polymer matrix. They also increase the basal distance facilitating the intercalation of monomers or polymer chains.
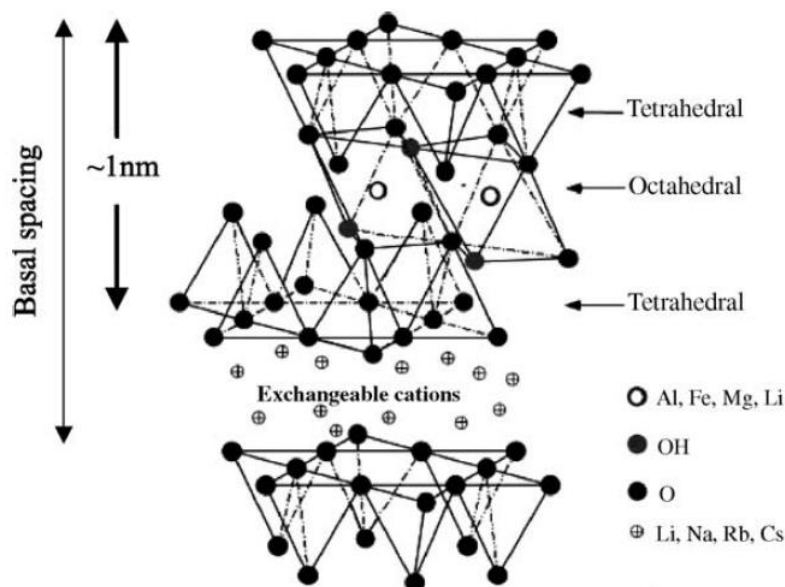
Figure 2. MMT structure [45].

On a larger scale, each MMT layer has a high aspect ratio lamella about 100-200 nm in length/width and 1 nm in thickness, as shown in Figure 3. Five to ten crystalline layers are associated by interlayer ions to form a primary particle, also called tactoid. The grey circles in the primary particle represent the intercalated cations and the lines represent the individual layers. These primary particles combine to form larger irregular aggregates (0.1-10 μm in diameter), which gives the clay its agglomerated structure.

Lamella	Primary particle	Aggregate
(1 nm)	(8 ~ 10 nm)	(0.1 ~ 10 μm)
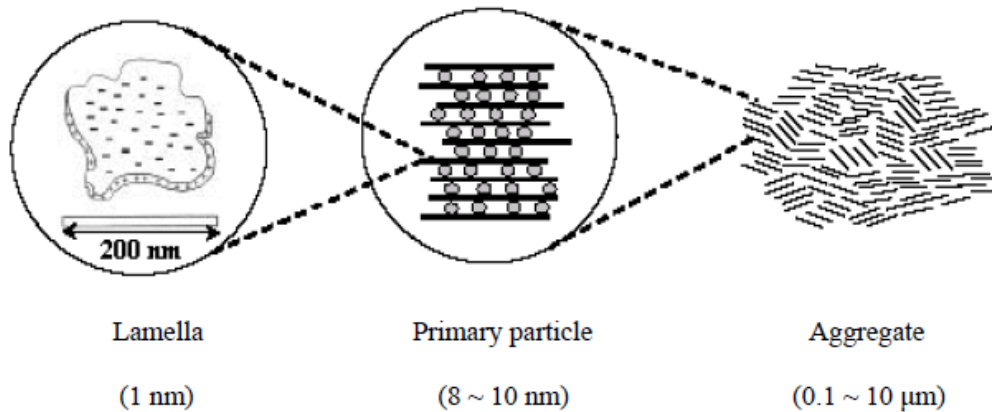
Figure 3. Model for the structure of MMT particles [46].

Polymer/MMT nanocomposites can present three different morphologies depending on the interfacial interactions between the polymer matrix and the MMT surface as shown in Figure 4. The three different possible morphologies are:

1) Similar to conventional composites: It occurs when the polymer does not enter the galleries and the MMT basal distance remains unchanged maintaining its tactoid structure (Figure 4 (a)).

2) Intercalated: It occurs when the polymer enters the galleries, increasing the basal distance, but keeping the tactoid structure (Figure 4 (b)).

3) Exfoliated: It occurs when the clay layers are completely pushed apart to create a completely disordered array (Figure 4 (c)).

Polymer/MMT nanocomposites can present a combination of all of these morphologies.

2.3 Polypropylene (PP)

PP is one of the most used and fastest growing classes of thermoplastics [47]. PP is produced by the polymerization of propylene, using a catalyst, into long polymer chains. The properties of PP in the molten state are related to molecular weight and

molecular weight distribution. In the solid state, the main properties of PP reflect the type and amount of the crystalline and amorphous phases [48]. The relative amount of each of these phases depends on structural and stereochemical characteristics of the polymer chains and the conditions under which the polymer is processed into the final products.
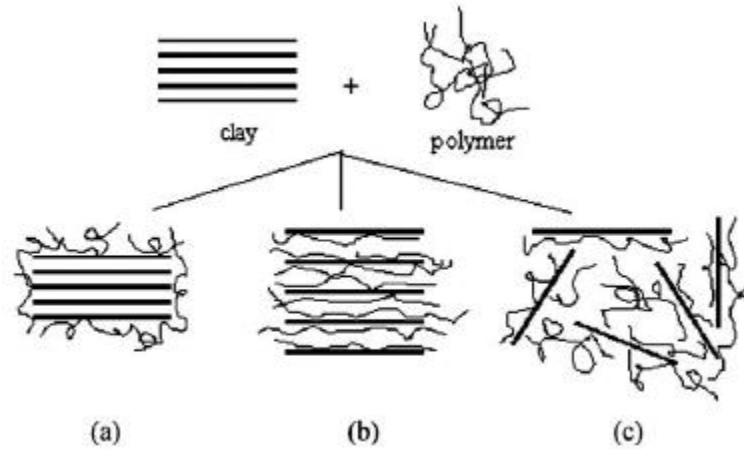
Figure 4. Schematic representation of different morphologies presented by polymer/MMT nanocomposites [49].

Regarding the stereochemical configuration of the propylene monomers, PP can be synthetized in three different configurations: atactic (aPP), syndiotactic (sPP), and isotactic (iPP) as shown in Figure 5. The isotactic PP has all the methyl groups located on the same side of the polymer backbone. In the syndiotactic PP, the methyl groups have alternate positions along the chain, while in the atactic configuration they are arranged randomly.
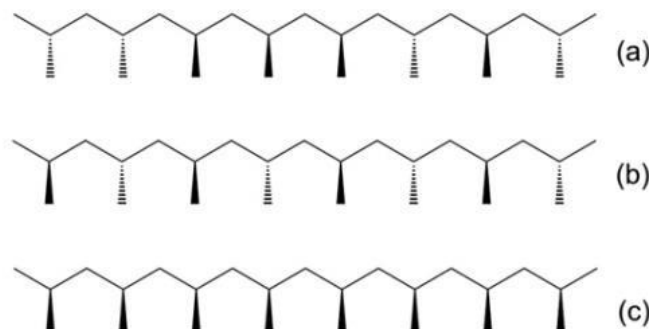
Figure 5. Stereochemistry of PP: atactic (a), syndiotactic (b), and isotactic (c).

9

Isotactic and syndiotactic polypropylene present stereoregularity, which allows the polymer chains to crystallize. The iPP is a semicrystalline polymer with good mechanical and thermal properties. This is by far the most used structure of PP. Syndiotactic PP is also semicrystalline with inferior mechanical and thermal properties; however, it presents excellent malleability, gloss and scratch resistance. The sPP is produced in relative small volumes and has limited applications [50]. Atactic PP is an amorphous material, waxy and slightly tacky, and mainly used as a component of hot melt adhesives and sealants [51].

There are three main processes used to produce PP in industrial scale [48]. The slurry process requires a solvent, usually a light hydrocarbon or heavier isoparaffins, to disperse the polymer produced in the reactor and to dissolve atactic byproducts. Although this technology has higher capital and operating costs, it produces PP with distinct properties, such as high polydispersity. Approximately 15% of the global production of PP still uses this technology.

The bulk process takes advantage of higher performing catalysts that do not produce atactic PP. It uses liquid propylene as the medium to the polymerization reaction and its main advantage is the high polymerization rate due to the high concentration of monomers. This process represents 60% of the global production of PP.

The gas-phase technology completely avoids the need for a solvent or liquid medium to disperse the reactants or products. This eliminates separation and recovery of solvents or liquid propylene required in the slurry or bulk reactors. The gas-phase supplies the monomer, it stirs the polymer particles and removes the heat from the reactor.

Several catalysts can be used to polymerize propylene, with the Ziegler-Natta catalyst being by far the most important. The importance of metallocene catalysts has been increasing in recent years; however, the third generation Ziegler-Natta catalyst is responsible for most PP production.

The Ziegler-Natta catalyst is a complex formed by reaction of a transition metal compound, usually titanium chloride, with a metal alkyl or alkyl halide, usually aluminum alkyls. The former is known as catalyst and the latter is the cocatalyst [52].

Ziegler-Natta catalysts are usually classified based in a historical perspective.

First Generation: Titanium chloride (δ–$TiCl_3$) activated by diethylaluminium chloride ($AlEt_2Cl$). The work of Karl Ziegler and Giulio Natta resulted in the first

commercial catalyst that was able to produce polypropylene with relatively high crystalline phase (90% insoluble in boiling heptane) [53]. This catalyst presented relatively low productivity (only the metal atoms on the surface of the catalyst are accessible to react with the cocatalyst) and the polymer needed deashing to neutralize residues of the catalyst.

The second generation of the Ziegler-Natta catalysts used $MgCl_2$ as support to increase the superficial area of the catalyst to increase the number active sites. This catalyst presented higher activity; however, they still produced a significant amount of atactic PP that needed to be removed.

The production of PP with substantially lower amounts of aPP was achieved by the third generation of Ziegler-Natta catalysts. Modifiers were added to the catalyst (internal donors) and to the cocatalyst (external donor). These modifiers increase the number of stereospecific active sites and selectively poison the non-stereospecific ones. The result is a catalyst with improved activity and stereospecificity. Deashing and atactic removal processes are not required, which simplifies the production. It is the catalytic system most used nowadays [54].

The fourth generation of Ziegler-Natta catalysts are the homogeneous single-site catalysts based on Al-oxane activated metallocene complexes. Metallocene catalysts can produce PP with controlled molecular structure, such as PP with narrow molecular weight distribution and syndiotactic PP. This class of catalyst had contributed significantly to understand the mechanism to polymerize olefins [55].

Furthermore, Ziegler-Natta catalysts have several types of active sites due to the intrinsic heterogeneity of the surface of the crystals where transition metals are deposited. The multisite nature of the catalyst is apparent in many ways: broad molecular weight distribution, polymer chains with different stereoregularity, copolymers with different composition, structural properties of the polymer chains can vary with time due to different activation and decaying times for different active sites, and selective poisoning of different active sites [56, 58].

2.4 Preparation of Polypropylene/Montmorillonite Nanocomposites

Several methods have been developed to prepare polymer/MMT nanocomposites. They can be divided into three main groups according to the starting materials and processing techniques [45]

2.4.1 Solution Blending

This method is based on the capacity of MMT, natural or modified, to swell in a proper solvent. This solvent can both swell/disperse the clay and dissolve the polymer under mixing and heating. After complete mixture, the solvent is removed by evaporation or the polymer/clay is precipitated by adding a non-solvent and the nanocomposite is obtained. The combination of solvent and clay modifier used with a specific polymer should be suitably chosen because, in some cases, the solvent can adsorb preferentially in the clay hindering the intercalation of the polymer molecules.

This method has been used mainly for water soluble polymers, such as poly(ethylene oxide) [59], polyamine, and poly(acrylic acid) [60]. However nanocomposites of hydrophobic polymer have also been prepared using this method. Qiu *et al*. [61] mixed linear low density polyethylene and a modified MMT in boiling xylene to obtain nanocomposites with 5 and 10%wt. They observed intercalation of polymer chains into the clay galleries and some layers were completely exfoliated. Chiu and Chu [13] mixed PP and several modified clays in 1,2,4-trichlorobenzene and, after the evaporation of the solvent, they obtained PP/MMT nanocomposites without the addition of compatibilizer. The clay was intercalated, partially exfoliated, and the material presented improved thermal stability.

2.4.2 Melt Processing

In this technique, no solvent is required and the clay is mixed with the polymer matrix in the molten state. A conventional processing method, such as extrusion, is used to mechanically mix the components and force the polymer chains into the clay galleries, eventually leading to exfoliation [62]. However, the intercalation only occurs if the polymer and clay present good affinity. This method presents several advantages, such as absence of solvent and use of conventional processing equipment, and is widely used in the preparation of nanocomposites [63]. Liu *et al.* [64] were the first to prepare polyamide 6/MMT nanocomposites using a twin screw extruder, but the material presented only partial exfoliation. Shortly after that, Dennis and coworkers [65] optimized the extrusion conditions and screw design to obtain highly exfoliated nanocomposites with different matrices.

Due to PP's easy processability, the melt processing was largely studied to prepare PP/MMT nanocomposites. However, PP is hydrophobic and presents very low

affinity with MMT (hydrophilic) forming an incompatible system. Several strategies have been used to increase the dispersion of the clay in the PP matrix, such as the use of organic modifiers in the clay [66, 67], addition of compatibilizers during processing [68, 73], and more exotic processing conditions such as ultrasound [74], electric fields [75] or clay suspensions [76]. Although some progress was made towards the exfoliation of MMT in PP, the dispersion levels are still far from those obtained using polar matrices, such as polyamides.

2.4.3 *In Situ* polymerization

For *in situ* polymerization, the liquid monomer, or monomer solution, is intercalated into the clay and then the polymerization is initiated. The polymerization can be initiated by heat, radiation, or a catalyst. Usuki *et al.* [3] successfully obtained exfoliated nanocomposites of nylon 6 and MMT by polymerizing ε-caprolactam in the interlayer space of the clay. This is also the method used to prepare thermosetting polymer/clay nanocomposites [19, 77, 78].

The preparation of PP/MMT nanocomposite by *in situ* polymerization has attracted more attention lately because it may overcome the barriers involved in the intercalation of hydrophobic PP chains into the galleries of the hydrophilic MMT using conventional methods. *In situ* polymerization of PP usually has three steps. First, the intercalation of the catalyst into the clay interlayer. Second, the clay is swelled with propylene, either in the bulk or slurry process (propylene solution). Finally the polymerization takes place.

Due to its defined structure, metallocene catalysts have been often used in the synthesis of PP/MMT nanocomposites using *in situ* polymerization. Tudor *et al.* [79] took advantage of the ion exchange capacity of selected layered silicates to intercalate a cationic catalyst, $[Zr(\eta\text{-}C_5H_5Me(thf)]^+$. The propylene polymerization was conducted after activation with methylaluminoxane (MAO); however, the catalyst was able to produce only aPP with low molecular mass. Yang *et al.* [16] used organically modified MMT containing OH groups to fix the MAO into the interlayer galleries. After intercalation of the catalyst and additional MAO for activation, this clay was used to polymerize propylene, as shown in Figure 6. This system presented fairly high activity to produce iPP, which led to good dispersion of the MMT.
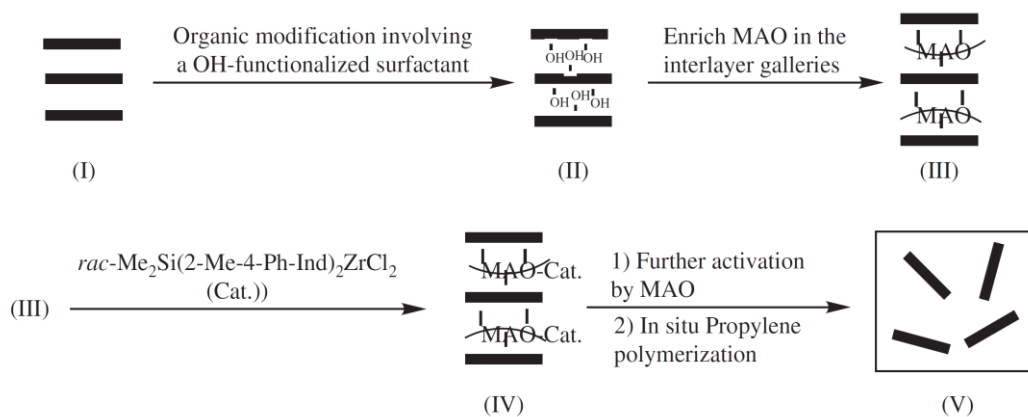
Figure 6. Scheme of the preparation of PP/MMT nanocomposites using intercalated catalyst [16].

Du *et al.* [80] used a similar approach to produce PP/MMT using conventional Ziegler-Natta catalyst. The authors used MMT modified with an imidazolium salt containing OH functional groups to fix $MgCl_2$ into the interlayer gallery followed by the addition of $TiCl_4$. The nanocomposites showed excellent dispersion of the clay; however, the improvement in mechanical properties was modest. Internal and external donors were also added to the catalyst system leading to the production of iPP with high isotactic index (insoluble in heptane); however, the crystallinity was relatively low for iPP (around 40%).

Although significant progress has been made in the synthesis of PP/MMT via *in situ* polymerization, a few problems still need to be overcome in order to produce nanocomposites at an industrial scale. Among them are poor adhesion between the clay and the polymer matrix, the reduced control of the polymer structure, and poor morphology of the polymer particle.

Recently, Dal Castel studied the preparation of PP/MMT nanocomposites using Ziegler-Natta catalysts with controlled morphology using the slurry process [17]. Under these conditions, the catalyst retained its characteristics, producing polymer particles with standard morphology and good dispersion of the clay. However, donors were not added to the catalyst and the PP obtained had a low isotactic index.

2.5 Properties of Nanocomposites

Polymer/MMT nanocomposites at low loading level of nanofillers often show notable improvements in numerous properties, such as Young's modulus, gas

permeability and thermal stability. Several methods have been used to model these properties [81] and a few of them will be presented in the following sections.

2.5.1 Mechanical Properties

One of the most significant achievements of the pioneering work of Usuki *et al.* [3] was an increase of 100% in the elastic modulus of a nylon 6 matrix containing only 4.2 wt.% of MMT. Several other authors reported significant increases in the modulus of polymer/MMT nanocomposites [82, 83]. The increment in the modulus in PP/MMT is usually more modest due to the nonpolar nature of PP. Svoboda *et al.* [84] reported an increase of 30% on the modulus of PP nanocomposites containing 5%wt. MMT.

The rule of mixtures is a very simple tool for modeling the mechanical behaviour of traditional composites. This model predicts that the elastic modulus of composites containing large particles should fall between an upper ($E_c(u)$) and lower ($E_c(l)$) bound represented by the following equations:

$$E_c(u) = E_m V_m + E_f V_f$$

$$E_c(l) = \frac{E_m E_f}{V_m E_f + V_f E_m}$$

Where E and V denote the elastic modulus and volume fraction, respectively, and the subscripts *c, m,* and *f* represent composite, matrix, and filler. Figure 7 presents experimental behaviour of a composite compared to the upper and lower bounds of the rule of mixtures [25]. It is possible to see in this figure that the combination of a filler with high modulus and matrix with low modulus results in a material with intermediate properties. Some authors suggest that the concept of matrix and filler, which are well established in conventional composites, cannot be applied directly in nanocomposites due to high surface area and small interparticle distances, creating a significant interfacial region with modified properties, as discussed in section 2.1.

However, several authors have been able to successfully predict the elastic modulus of polymer nanocomposites using conventional composites theory with the Halpin-Tsai and Mori-Tanaka models being often used [27, 85, 86]. Sheng *et al.* [87] used a finite elements method to describe the mechanical behaviour of polymer/clay nanocomposites. They observed a linear increase in the modulus of the material with the clay weight fraction (W_c), as shown in Figure 8. At a fixed loading, the reduction of the number of lamellae strongly increases the modulus of the material (Figure 8 (a)). The

increase in the intralamellar distance produces a more modest increase in the modulus (Figure 8 (b)).
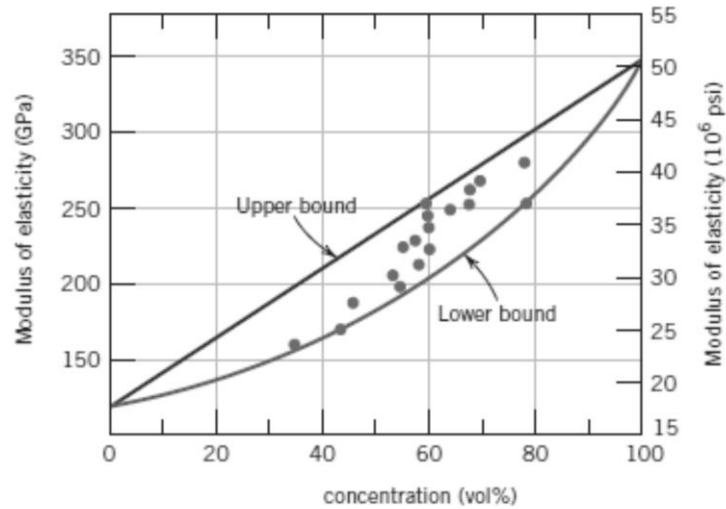
Figure 7. Modulus of elasticity versus volume percent for a composite. The points represent experimental values and lines are upper and lower bound according to equations above [25].
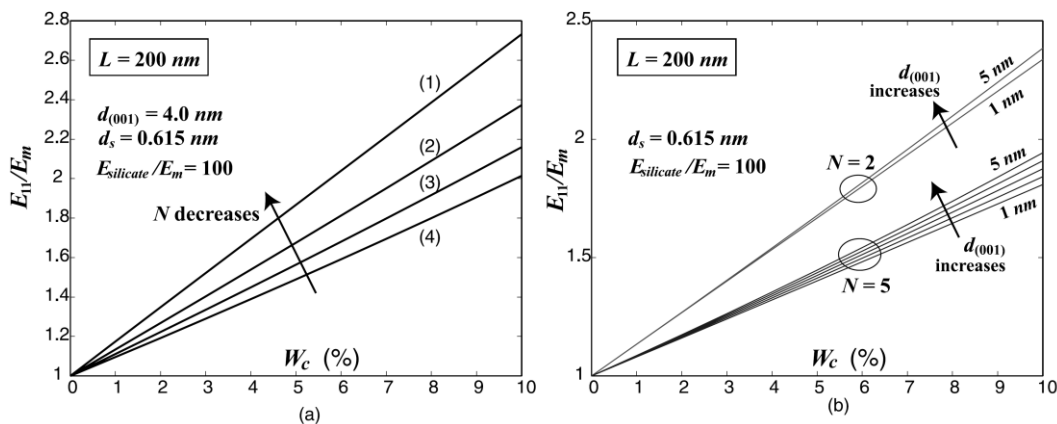
Figure 8. Effect of structural parameters on the modulus of polymer/clay nanocomposites. (a) Effect of the number of lamellae in a primary particle, N, at a fixed d_{001}; (b) Effect of d_{001} at two fixed values $N=2$ and $N=5$.

Heat distortion temperature (HDT) of a polymeric material is an index of heat resistance towards applied load and it is a property of interest for applications at high temperatures. Strong increases in the HDT of polymer nanocomposites are often reported. Kojima *et al.* [88] reported an increase of 90ºC in nylon 6/MMT

nanocomposites. PP/MMT containing 6%wt. of clay prepared by Nam *et al.* presented HDT of 152ºC, which is 43ºC higher than the pure PP [89]. The increase in HDT reflects the increase in the material modulus over a broad temperature range, as shown by Fornes and Paul when modeling the properties of nylon 6/MMT nanocomposites(Figure 9) [27].
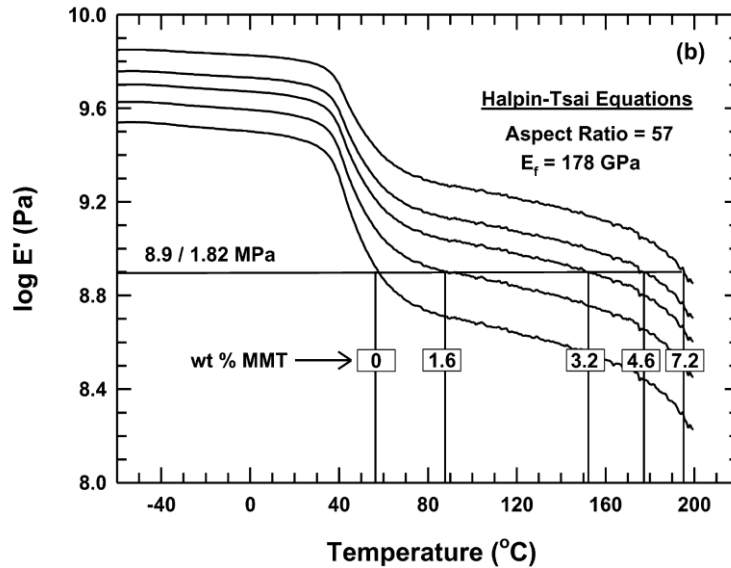
Figure 9. Storage modulus versus temperature of nylon 6/MMT nanocomposites containing different loadings (1.82MPa represents the modulus of the material at the HDT) [27].

2.5.2 Gas Barrier Properties

Polymer/MMT nanocomposites present improved gas barrier properties because the clay imposes a restriction to the gas diffusion. The clay lamellae are impermeable to gases, creating a maze or tortuous paths that retard the progress of the gas molecules through the polymer matrix. This effect is shown in Figure 10.

The Nielson model and its modified versions have been used successfully to describe the increase in the gas permeability of lamellar nanocomposites [90, 91]. According to this model [92], the permeability coefficient (P_c/P_p) of lamellar filler dispersed and completely aligned (all filler has their larger surface parallel to the film surfaces, but there is no order in the filler center of mass) is defined as:

$$\frac{P_c}{P_p} = \frac{1 - V_f}{1 + aV_f}$$

17

Where P_c and P_p, is the permeability of the composite and the polymer respectively, V_f is the filler volumetric fraction and a is the filler aspect ratio ($a=l/2d$ for square fillers). Bharadwaj [93] modified this equation to account for non-aligned fillers, by introducing an order parameter S for the filler orientation, which reduces to the Nielsen equation for perfectly aligned fillers ($S=1$):

$$\frac{P_c}{P_p} = \frac{1-V_f}{1+aV_f\frac{2}{3}\left(S+\frac{1}{2}\right)} \quad \text{with} \quad S = \frac{1}{2}(3\cos 2\theta - 1) = \begin{Bmatrix} 1 & \text{II surface} \\ 0 & \text{random} \\ -1/2 & \perp \text{surface} \end{Bmatrix}$$

Based on this model, it is possible to see that the permeability depends on the loading, aspect ratio, and orientation of the filler.
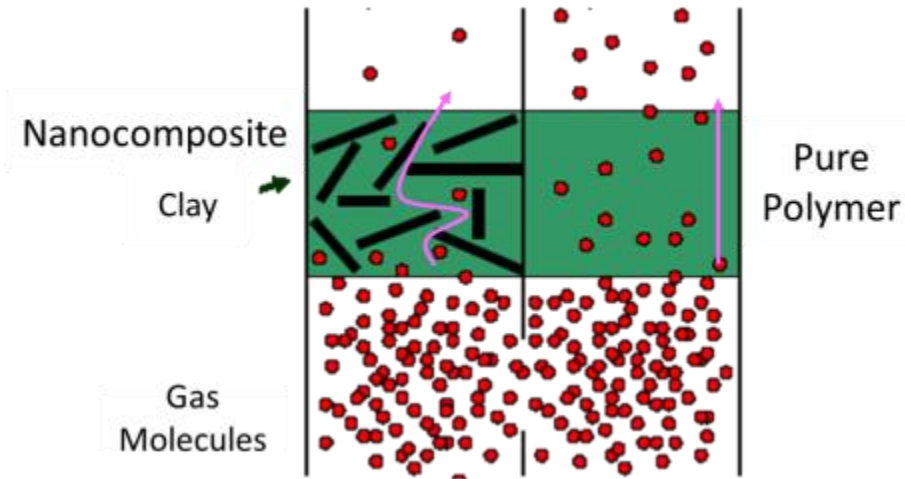
Figure 10. Formation of tortuous path in polymer/MMT nanocomposites.

Nanocomposites often present improved thermal stability when the material is analysed by thermogravimetric analysis (TGA), with several authors reporting an increase in the temperature of degradation of the nanocomposites [94, 97]. This effect is also a consequence of the tortuous path created by the clay. However in this case, the lamellae obstruct the release of the gases generated by the decomposition of the polymer [97].

2.6 Supercritical Fluids

2.6.1 Supercritical Fluid and Properties

A supercritical fluid (SCF) can be defined as a substance with a temperature and pressure above its critical point (critical temperature, T_{sc}, and critical pressure, P_{sc}), where distinct liquid and gas phases do not exist. Critical temperature is the highest temperature at which a pure substance can exist in gas/liquid equilibrium.

Supercritical fluids possess unique properties such as density control, solvating power, low viscosity, high diffusivity, near zero surface tension among others [98]. Table 1 shows a range of selected properties of supercritical fluids to illustrate that they exhibit properties between liquid and gas phases.

Table 1. Properties of fluids in different states [99]

	Density (g/mL)	Dynamic Viscosity (g/cm-sec)	Diffusion Coefficient (cm^2/sec)
Gas (ambient)	0.0006-0.002	0.0001-0.003	0.1-0.4
Supercritical Fluid (T_{sc}, P_{sc})	0.2-0.5	0.0001-0.0003	0.0007
Liquid (ambient)	0.6-1.6	0.002-0.03	0.000002-0.00002

The supercritical point and properties of some selected substances are presented in Table 2.

Thermodynamics properties of a substance are usually represented in tables or diagrams where the abscissa and ordinate represents physical properties, such as enthalpy, temperature, entropy or volume.

A phase diagram is a tool used to observe the substance phases according to their pressure and temperature condition. For example, Figure 11 shows a carbon dioxide pressure-temperature phase diagram.

The most well-known and used is the Mollier diagram, where the abscissa represents the enthalpy and the ordinate represents the pressure. Figure 12 shows a schematic Mollier diagram that identifies the critical point and supercritical region, as well as the liquid and gas phases.

Table 2. Critical point of selected substances.

Fluid [100-103]	Molecular weight (g/mol)	T_{sc} (°C)	P_{sc} (bar)	Crititcal Density (Kg/m^3)
Acetone	58.08	235.10	48.00	278.00
Ammonia	17.03	132.40	111.30	255.00
Carbon dioxide	44.01	31.00	72.90	467.60
Chlorobenzene	112.56	359.00	45.20	
Chlorodifluoromethane(R22)	84.47	96.40	48.50	523.84
Cyclohexane	84.16	281.00	40.70	
Ethane	30.07	32.17	48.70	206.18
Ethanol	46.07	240.90	60.60	276.00
Ethylene	28.05	9.20	50.42	214.20
Methanol	32.04	239.60	79.80	272.00
n-Hexane	86.18	234.34	30.18	233.00
Propane	44.10	96.74	42.51	220.48
Propylene	42.08	91.06	45.55	230.08
Toluene	92.14	318.64	41.09	291.00
Trichlorofluoromethane (R11)	137.37	197.60	44.17	619.44
Water	18.02	374	217.7	322
Xenon	16.59	58.42	131.29	1102.9

A complete Mollier diagram for propylene is show in Figure 13. The advantage of using a Mollier diagram is that various thermodynamic information can be found in one place (temperature, pressure, enthalpy, entropy, specific volume and phase regions). Using the Mollier diagram, it is also possible to find the thermodynamic pathway from one state to another.
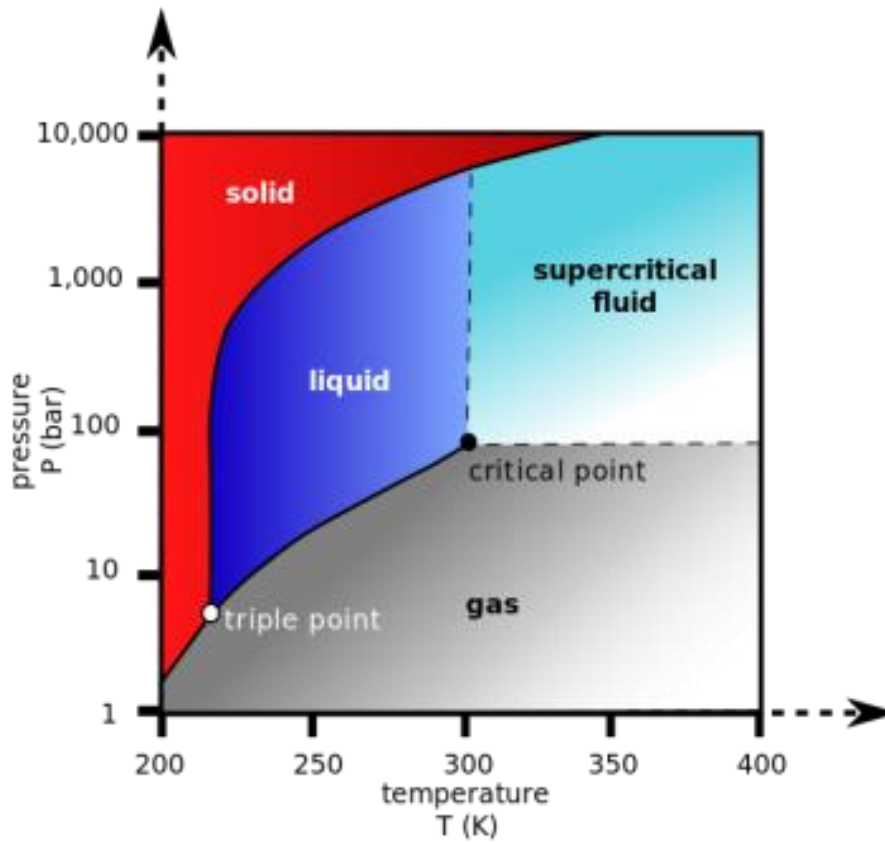
Figure 11. Phase diagram for CO_2,
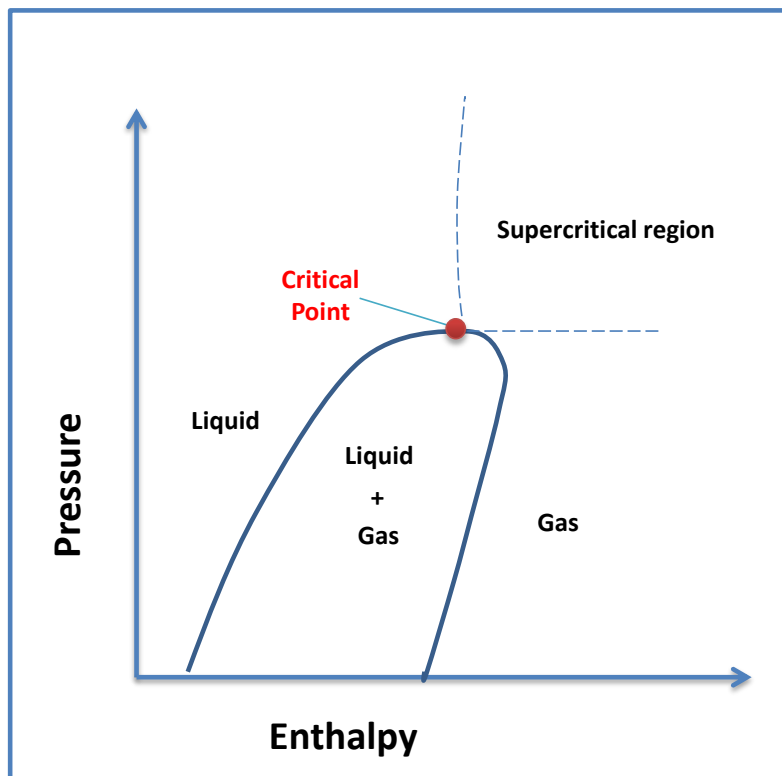
Figure 12. Schematic Mollier diagram.
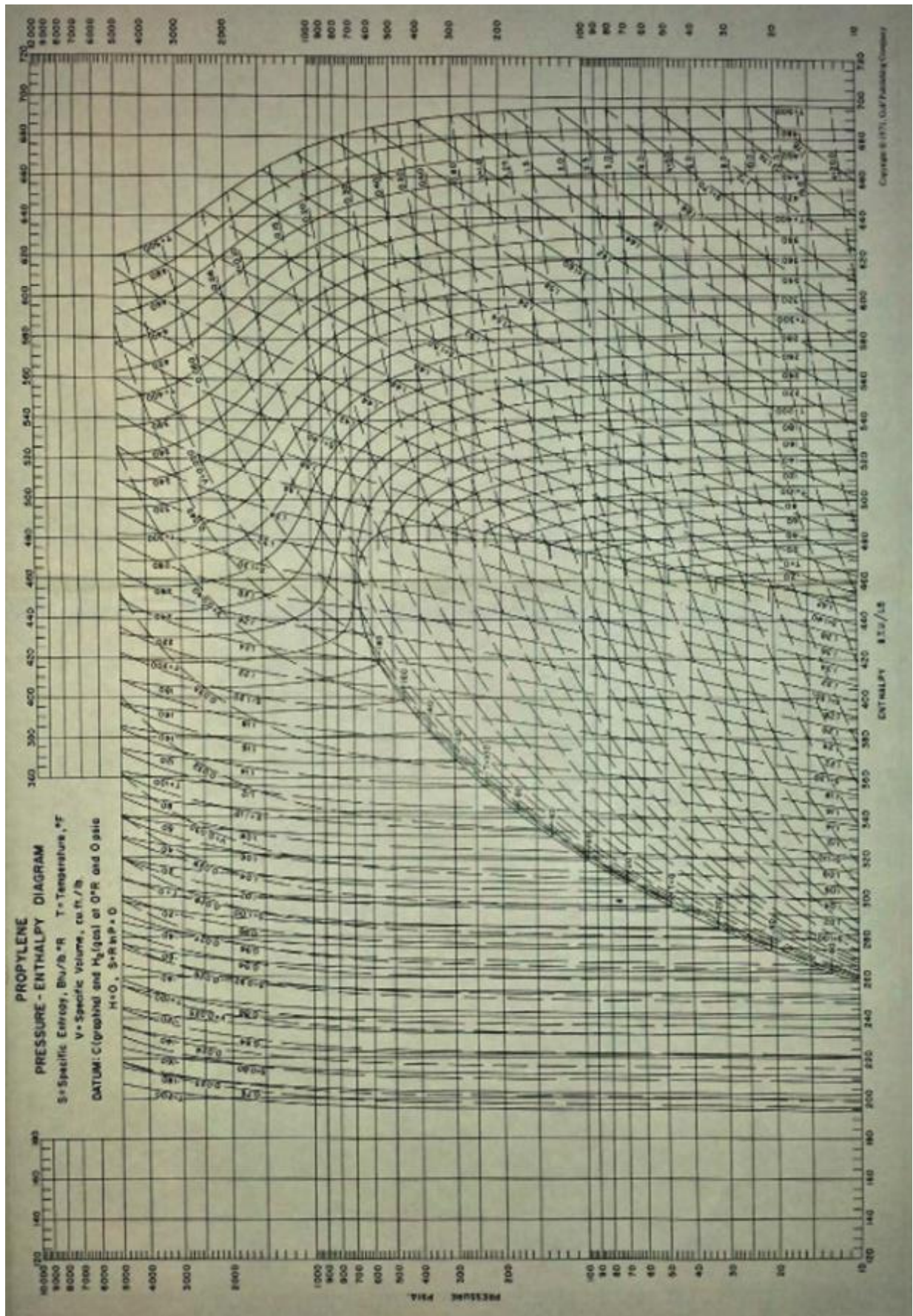
Figure 13. Mollier diagram for propylene.

22

2.6.2 Using SCF as an Auxiliary Method to Produce PP/MMT Nanocomposites

The mass transfer rates in SCF are considerably faster than that of the liquid solvent. The solvent power of a SCF is a function of its density and it can be fine-tuned by changing the temperature and pressure conditions. In general, the solubility of a solute in a SCF increases with the pressure at constant temperature due to the increase in density. At constant pressure, the effect of temperature on the solubility is more complex. Increasing the temperature can lead to lower solubility due to a reduction in density; however, higher temperatures can also increase the solubility due to an increase in the kinetic energy of the system and consequently the solvent power of the SCF [98].

Various research groups have explored the distinctive properties of SCF, mainly supercritical CO_2, to obtain polymer nanocomposites using melt extrusion. Only one report in the open literature has described the use of supercritical propylene to obtain polymer nanocomposites using *in situ* polymerization.

2.6.3 Use of SCF in the Melt Extrusion Method

Ma *et al.* prepared PP/sepiolite nanocomposites using supercritical CO_2 assisted mixing. The results showed improved dispersion of the nanofiller and consequently improved mechanical properties when compared with a traditional melt compounding method [104]. The authors suggested that the lower melt viscosity was responsible for reducing the breakage and improving the dispersion of the nanofiller. Hwang *et al.* [105] used supercritical CO_2 to improve the dispersion of MMT in PP nanocomposites prepared using twin screw extrusion, as shown in Figure 14. They observed improved thermal and mechanical properties when using the SCF. Even though the aforementioned process is distinct from the process to be utilized in this work, it worth noting since it explains the use of SCF in producing nanocomposites.

On the other hand, Yang and Ozisik investigated the effect of different SCFs on the dispersion of nylon 6/MMT nanocomposites prepared by extrusion and did not observe improved clay dispersion due to the lower melt viscosity when using SCF [106].

Another strategy was used by Manke *et al.* to produce PP reinforced by MMT [24]. In this process, the clay is swelled with supercritical CO_2 in a pressurized vessel and then catastrophically depressurized into another vessel at atmospheric pressure, so that the stacked clay layers are forced apart. The inventors claimed that the clay was

23

properly individually dispersed after the depressurization; however, they did not provide any mechanism for assuring that the clay would remain exfoliated after being mixed with the polymer. Kannan *et al.* [107] studied this process in more detail and observed that the degree of dispersion of the clay after depressurization varies with the CO_2-philicity of the clay. Significant dispersion was achieved with an organically modified clay (Cloisite 93A), whereas little to no dispersion was achieved for Cloisite Na^+ (CO_2-phobic).
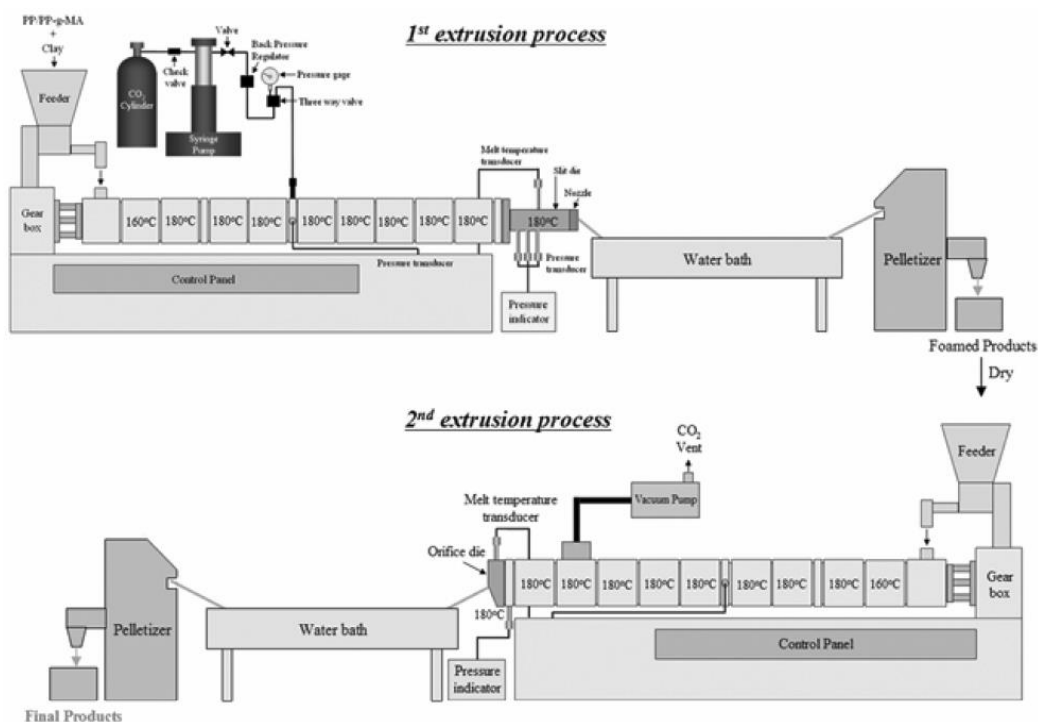
Figure 14. Schematic of Supercritical CO_2 Assisted Twin Screw Extrusion Process [105].

Although CO_2 has some advantages when used as a SCF, it cannot be used for the method of *in situ* polymerization of polypropylene because it can coordinate to the transition metal in the Ziegler-Natta catalyst stopping the polymer chain from growing (coordinative poison) [108].

2.6.4 Use of SCF in the *in situ* Polymerization Method

Liberman and coworkers (including the author of this thesis) described the utilization of supercritical fluid for the preparation of nanocomposites of polypropylene and montmorillonite [109]. In this method, the clay was dried and then treated in propylene near supercritical conditions for four hours. This mixture was de-pressurized

in inside a reactor where the polymerization of propylene, catalyzed by a Zigler-Natta catalyst, was conducted. Polypropylene nanocomposites containing 2 to 3 wt.% MMT were produced using this method. These nanocomposites had improved flexural modulus, impact strength, heat distortion temperature and hardness. Although the method was successful in producing nanocomposites with improved properties, the authors provided only a few examples and did not explore the effect of different conditions of temperature and pressure within the supercritical propylene.

2.7 LITERATURE GAP

To the best knowledge of the author of this thesis, there is no report in the open literature, other than the one from Liberman and coworkers [109], using propylene as a supercritical fluid for the preparation of polypropylene-clay nanocomposites. This is identified as a gap in the literature because supercritical propylene can be obtained at relatively mild temperature and pressure conditions presenting a great potential as the dispersion medium of the clay and subsequent application in the preparation of polypropylene-clay nanocomposites using the *in situ* polymerization method.

Furthermore, supercritical propylene could potentially be used as the reaction medium for the polymerization in a method similar to the bulk process. However, the average activity of the catalysts usually decreases at temperatures above 80ºC due to the instability of the catalyst. The temperature required for achieving the supercritical condition (91°C) is above the typical polymerization temperature ($< 80^{o}$C). Higher temperatures during the polymerization also reduce the average molecular weight of the PP [110] and decrease the mechanical properties of polypropylene in general.

3 MATERIALS AND METHODS

3.1 Materials

Six montmorillonites (MMTs) were supplied by Southern Clay Products, Inc. (Cloisite) and two by Nanocor. These clays have reported cation exchange capacity of 92mEq/100g and their original cations were exchanged by sodium (cloisite Na+) or quaternary ammonium salts, as shown in Table 3.

Table 3. Characteristics of the clay modifiers.
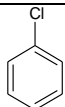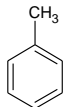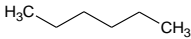
Clay	Quaternary ammonium salt	Amount of modifier (mEq/100g)	Structure of the modifier
Cloisite Na+	-	-	-
Cloisite 30B	methyl bis-2-hydroxyethyl alkyl	90	
Cloisite 10A	dimethyl benzyl alkyl	125	
Cloisite 93A	dimethyl alkyl	90	
Cloisite 20A	dimethyl dialkyl	95	
Cloisite 15A	dimethyl dialkyl	125	
Nanomer I.44P	dimethyl dialkyl	35-45wt.%	
Nanomer I.31PS	octadecylamine	15-35wt.%	
	aminopropyltrytriethoxysilane	0.5-5wt.%	

*alkyl – C_{14}-C16-C_{18}

Solvents used in the swelling tests were purchased from Sigma-Aldrich Co. and were used as received. The properties of the solvents are presented in Table 4. Toluene

used in the polymerization reactions was dried using a solvent purification system from MBraum Inc to achieve low level of water (< 5 ppm).

Table 4. Properties of the solvents.

Solvent	Structure	Molar mass (g/mol)	Density (g/mL)	Relative polarity [111]	Melting Point (ºC)	Boiling Point (ºC)
Chlorobenzene		112.56	1.11	0.188	-45	131
Toluene		92.14	0.870	0.099	-95	111
Cyclohexane		84.16	0.778	0.006	7	81
n-Hexane		86.18	0.654	0.009	-95	69

Propylene (polymerization grade) and nitrogen (ultra-high purity grade, 5.0) were supplied by Praxair, Inc. and they were dried through a column containing molecular sieves 3A and deoxygenated using a column containing a copper catalyst.

The Lynx 1000 propylene catalyst from Basf Inc. was supplied by Braskem America and used as received. It is a Ziegler-Natta catalyst supported in magnesium chloride ($MgCl_2/TiCl_4$) suspended in mineral oil (20%wt.). The solid fraction has a titanium content of 2.5%wt. Triethylaluminum was used as cocatalyst. It was supplied by Sigma-Aldrich Co. as a solution of 1mol/L in hexane. Dicyclopentyldimetoxysilane (Gelest, Inc.) was added to the triethylaluminum solution to work as external donor. The Al:donor ratio was 20:1.

The materials for assembling the high pressure system to handle the supercritical fluid were supplied by Autoclave and the parts list can be found in Appendix A.

3.2 Preparation of Nanocomposites

PP polymerizations were conducted in a stainless steel stirred reactor (Paar Instrument Co.) connected to a pressure vessel where liquid propylene was heated above the supercrital temperature.

The reactor was dried and purged three times with nitrogen. Subsequently, 500mL of dried toluene was added and the temperature was raised to 60ºC. The

cocatalyst (15mmol of triethylaluminum and 0.75mmol of dicyclopentyldimetoxysilane) was added under intense stirring. Once the temperature was stable (± 1ºC), the catalyst (0.10mmol of Ti) was added to the reactor and the propylene polymerization was carried out at propylene partial pressure of 70psi. After one hour, the monomer pressure was released and the polymer slurry was precipitated in 500mL of ethanol. The suspension was filtered with paper filter and washed with 100mL of ethanol twice. Finally, the polymer was dried in a vacuum oven at 70ºC overnight.

For the reactions that used clays, the clays were added following two different procedures, as outlined below:

-Without supercritical pre-treatment: the clays (2.0g) were dried under vacuum at 80ºC overnight and then transferred to a Schlenk tube which was later purged three times with nitrogen and vacuum cycles. Dry toluene (500mL) was added and the clay swelled for 1 hour under intense stirring. The swollen clay was transferred to the reactor before adding the dried toluene as previously described.

-With supercritical pre-treatment: the clays (2.0g) were dried under vacuum at 80ºC overnight and then transferred to the transfer vessel which was later purged three times with nitrogen and then vacuum was applied. This transfer vessel was then connected to the propylene tank and to the pressure vessel, which was also previously purged. A specific amount of liquid propylene (as determined in Section 4.2) was transferred from the propylene tank to the transporting vessel and then to the pressure vessel. The clay was carried between the vessels by the propylene flow. The temperature was slowly increased until reaching a specific temperature and correlated pressure. The mixture of supercritical propylene and clay was held at the specific temperature and pressure for 30 minutes. Then this mixture was abruptly released in the reactor immediately after adding the catalyst and the polymerization was carried out as previously described. The schematic drawing of the pressure vessel used to achieve the supercritical conditions is presented in Appendix B.

3.3 Characterization Methods

3.3.1 Transmission Electron Microscopy

Transmission electron microscopy (TEM) was used to investigate the nanoscale morphology of the samples. The nanocomposite samples were embedded in epoxy resin

and cured for 24 hours before being cut with the ultramicrotome. The cuts, in the range of 70-100 nm, were obtained using an ultramicrotome Leica EM UC6 fitted with a diamond knife (Diatome, Ltd.). The cuts were then mounted on a copper grid (400 mesh). A Phillips CM10 transmission microscope, operating at 80kV, was used.

3.3.2 X-ray Diffraction

The X-ray diffraction (XRD) patterns were obtained with a D8-ADVANCE powder X-ray diffractometer (Bruker, Inc.) in the reflection mode operating at 40 kV and 30 mA. The incident radiation was Cu Kα with a wavelength of 1.54Å. The clay samples were in powder form and the polymer samples were in the film form (preparation described in the item 3.3.3). The interlamellar distance, d_{001}, of the clay was calculated using Bragg's Law:

$$d = \frac{\lambda.n}{2.sen\theta}$$

Where d is the spacing between the planes in the atomic lattice, λ is the wavelength of the incident radiation, θ is the angle between the incident ray and the scattering planes, and n is an integer number.

3.3.3 Differential Scanning Calorimetry

Differential scanning calorimetry (DSC) was carried out in a DSC model Q20 from TA Instruments using nitrogen atmosphere and approximately 6mg of sample in film form. The films were prepared by heating around 200mg of the sample at 190°C for one minute and pressing it for two minutes with six metric tons.

The samples were analyzed by heating them to 200ºC for five minutes to eliminate the thermal history of the material and then cooled at 10ºC/min to 50ºC. The crystallization temperature (T_c) was defined as the peak maximum during this cooling cycle. After an isothermal period of five minutes, the samples were heated at 10ºC/min to 200ºC. The melting temperature (T_m) and enthalpy of fusion (ΔH_m) were defined as the peak maximum and the peak area, respectively, during this heating cycle.

The crystallinity of the PP matrix was measured using the following equation:

$$\chi_c = \frac{\Delta H_m}{f_p \Delta H_m^0} \times 100$$

where ΔH_m is the enthalpy of fusion of the sample, f_p is the mass fraction of PP in the sample and ΔH^0_m is the enthalpy of fusion of PP 100% crystalline (207.1J/g) [112].

3.3.4 Thermogravimetric Analysis

The thermal stability and clay loading of the nanocomposites were measured using thermogravimetric analysis (TGA) using a TGA Q50 (TA instruments) under nitrogen atmosphere. The samples were heated at 20ºC/min to 800ºC.

The clay loading was calculated using the following equation:

$$loading(\%) = \frac{N_r}{C_r} * 100$$

where N_r is the nanocomposite residue at 800ºC and C_r is the pure clay residue at 800ºC.

3.3.5 Infrared Spectroscopy

Polymer samples were analyzed by Fourier Transform Infrared Spectroscopy (FTIR) as films. The films were prepared by heating around 50mg of the sample at 190°C for 30 seconds and pressing it for one minute with 18 metric tons. After a conditioning period of seven days at room temperature, the infrared spectra of the films were recorded using a computer-aided Bruker Tensor 27 (Bruker Co.) FTIR system. The spectra were obtained with transmission through the films with units in transmission mode in the range from 400 to 4000cm^{-1}, after 32 scans, with a resolution of 4cm^{-1}.

3.3.6 Scanning Electron Microscopy

The morphology of the samples was analyzed by scanning electron microscopy (SEM) using a Zeiss LEO 1530 Gemini microscope operating at 10kV. The samples were placed on conductive tapes on the aluminum pan and were coated in 10 nm thick gold film using high vacuum sputter.

3.3.7 Clay Swelling Test

The clay swelling tests were performed with a modification of the method described by Foster [113]. Here, 2g of clay were transferred to a graduated cylinder following the addition of 50mL of solvent. Two different methods were used in order to

mix the suspension: manual stirring and ultrasonic bath (Branson model 1510) overnight (approximately 15 hours).

The ratio between the volumes occupied by the clay to the total volume in the graduated cylinder was observed after different settling times, ranging from 5 minutes to 28 days.

4 RESULTS AND DISCUSSION

This study contains three parts:

- clay swelling,
- supercritical conditions, and
- *in situ* polymerization.

4.1 Clay Swelling

This part of the study used a slurry polymerization process to produce PP without assistance of supercritical fluid. Although several examples of solvent-clay have been reported in the literature, there are no reports comparing systematically clays and solvents that are relevant for *in situ* polymerization. These experiments were performed here to evaluate the compatibility among different clays and solvents.

The swelling behavior of unmodified MMT (Cloisite Na+) and the other seven clays (Table 3) were tested in four organic solvents (Table 4). Except for chlorobenzene, all of the others solvents are suitable to propylene polymerization.

Chlorobenzene is a solvent slightly more polar than toluene and although it is not suitable as a medium to propylene polymerization using Ziegler Natta catalysts, it was evaluated to provide a comparison between polar and non-polar solvents on clay swelling.

Figure 15 presents the swelling behavior of different clays in chlorobenzene following two different protocols, as described in section 3.3.7. The swelling behavior was measured with Volume Ratio calculated between the volumes occupied by the clay to the total volume of the system in the graduated cylinder. Selected images of these systems are included in the Appendix C. In general the following behaviors were observed:

- *poor interaction* of the clay with the solvent – observed by fast settling of the clay and low Volume Ratio;
- *good swelling* of the clay by the solvent – observed by increased Volume Ratio and with or without two distinct regions;
- *exceptional swelling* of the clay – observed by clay occupying the entire volume in the system, only one homogeneous region, and creating a translucent system.
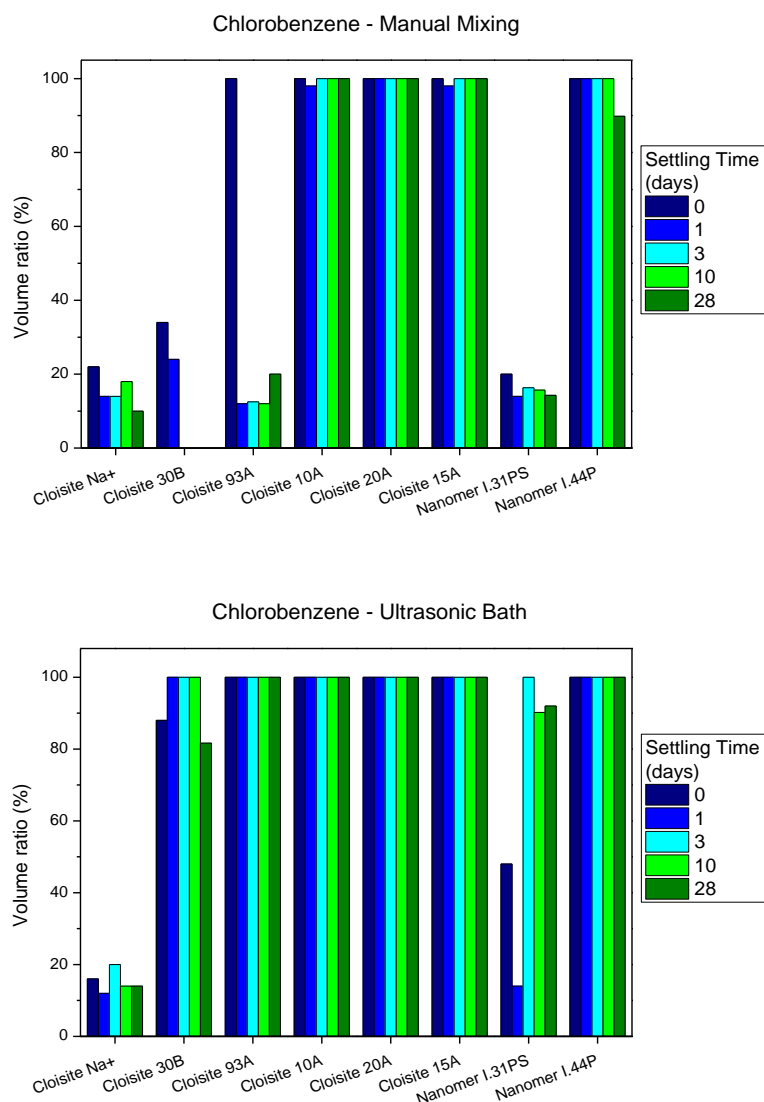
Figure 15. Swelling behaviour of different clays in chlorobenzene.

It is possible to see that clays with stronger polar character, such as Cloisite Na$^+$ and Nanomer I.31PS, have limited swelling in this solvent. The clays Cloisite 30B and 93A presented interesting behavior, showing poor swelling with manual mixing, but once sonicated, they presented very strong swelling and stability over time. These results suggest that these clays have an intermediate polarity when compared with the other clays used in this work. The clays Cloisite 10A, Cloisite 20A, Cloisite 15A, and Nanomer I.44P were easily swollen by the solvent using either of the mixing conditions, forming a stable suspension for several days.

Toluene presents relatively low polarity and was previously used for the synthesis of nanocomposites via *in situ* polymerization [17]. Figure 16 presents the behaviour of the clays in toluene. When non-polar clays were suspended in toluene

using manual mixing, a homogeneous suspension was formed; however, this suspension was not stable and after a few days the clay precipitated. The use of an ultrasonic bath strongly increased the swelling of the clay, forming stable suspensions even for clays with a more polar character, such as Cloisite 30B and Nanomer I.31PS. Toluene was not able to swell the unmodified clay.
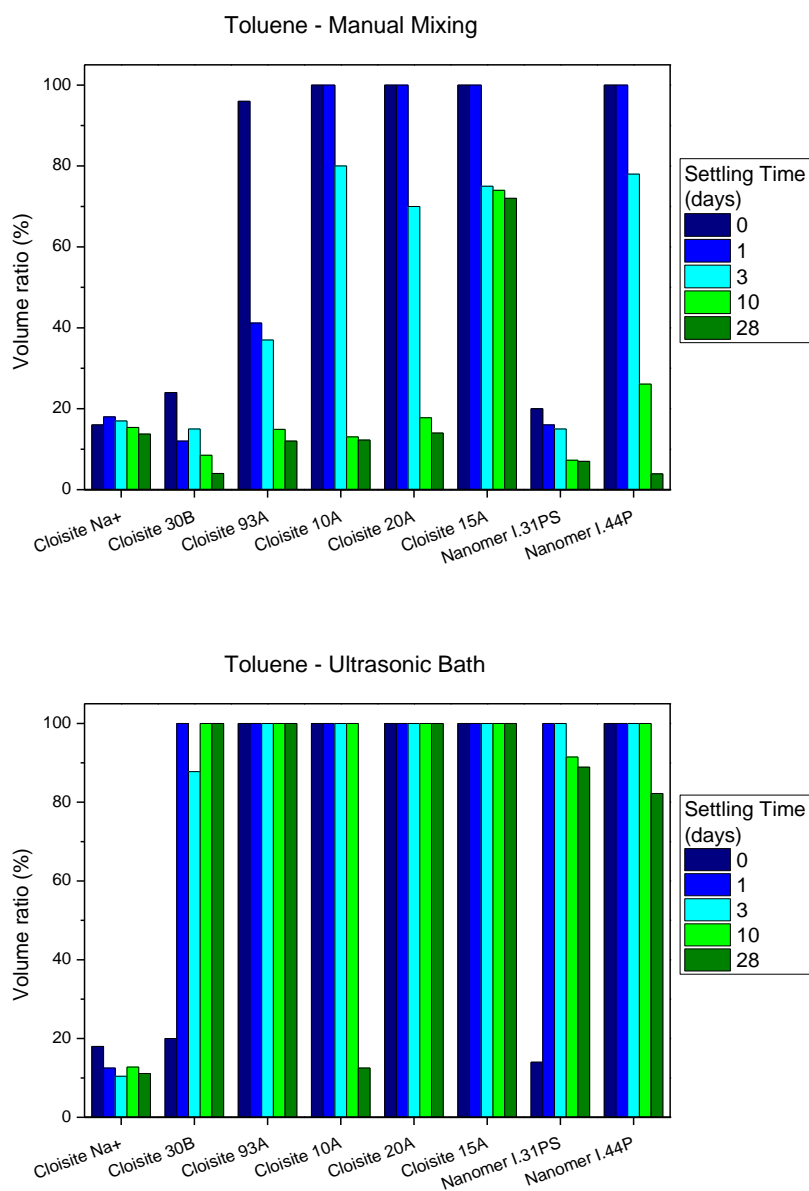
Figure 16. Swelling behaviour of different clays in toluene.

Cyclohexane was also tested to serve as a solvent for the polymerization of PP. As shown in Figure 17, only Cloisite 15A formed a good suspension in cyclohexane using manual mixing, although it was not completely stable. The use of an ultrasonic bath promoted a better dispersion of the clay and yielded a stable suspension. The

ultrasonic bath also promoted better dispersion of the clays: Cloisite 93A, Cloisite 20A, Cloisite 15A, and Nanomer I.44; however, these suspensions had limited stability, indicating weak clay/solvent interaction.
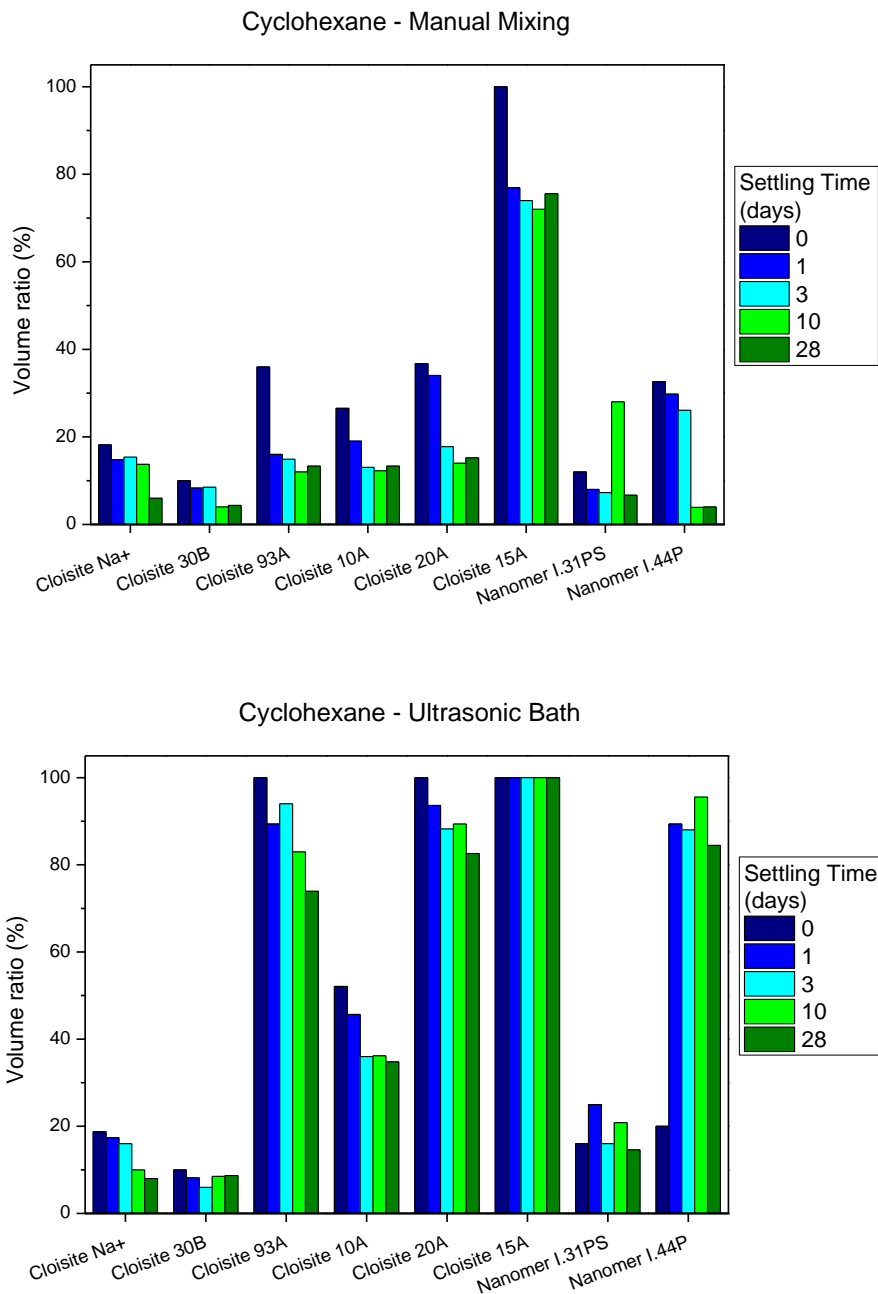
Figure 17. Swelling behaviour of different clays in cyclohexane.

Hexane is the solvent most commonly used in the polymerization of PP in the slurry process; however, this solvent has very poor compatibility with MMT, as shown in Figure 18, making it unsuitable to conduct the *in situ* polymerization of PP/MMT nanocomposites.
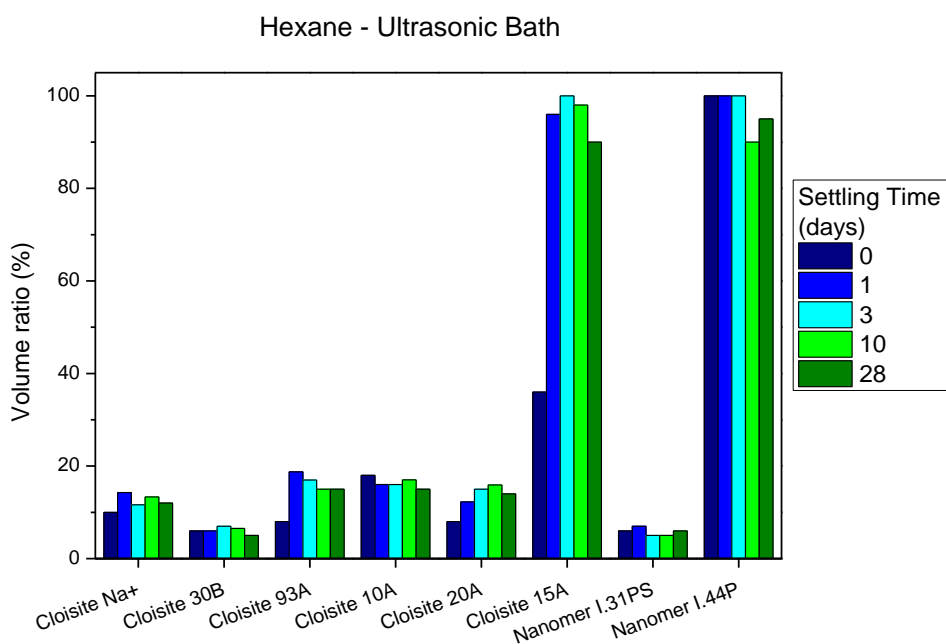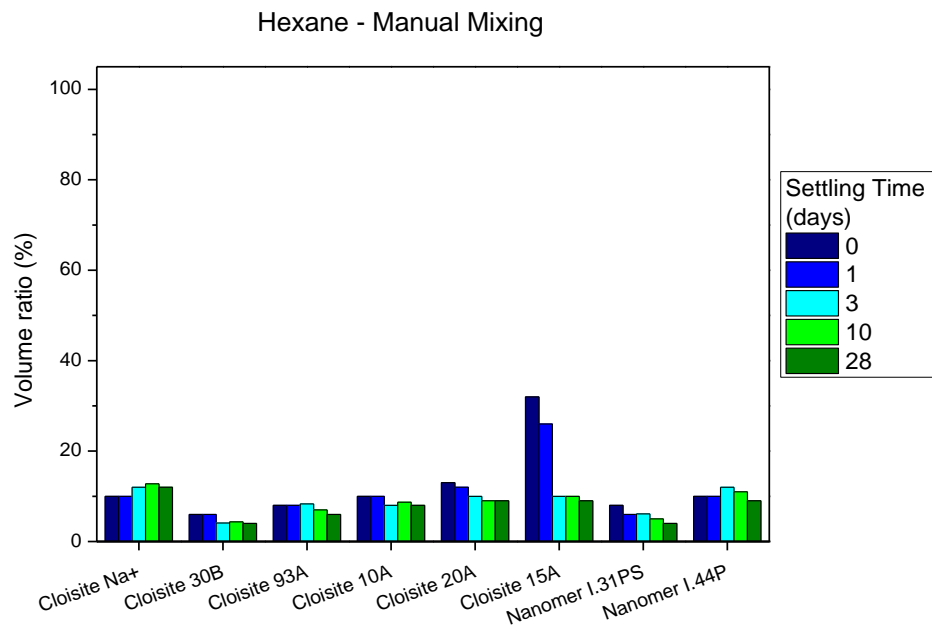
Figure 18. Swelling behaviour of different clays in hexane.

The results from the swelling behaviour of the clays in different solvents indicate that solvents with some polarity, such as chlorobenzene and toluene, are better at producing a stable suspension of the clay. Toluene represents the best option because chlorobenzene has more limitations with respect to propylene polymerization using Ziegler Natta catalysts.

When looking at the behaviour of the clays, it is possible to see that the clays Cloisite 15A and Nanomer I.44P are the most compatible with nonpolar solvents. These clays are produced by different companies, but use the same organic modifier and have very similar specifications (Table 3). Since the Cloisite 15A resulted in slightly superior swelling in toluene, when compared with Nanomer I.44P, this clay will be used for polymerization reactions later in this work.

Cloisite 93A also presented fairly good swelling in toluene and it presented good results in the preparation of PP/MMT nanocomposites using *in situ* polymerization as shown by other authors [17, 114].

In conclusion, Cloisite 15A and Cloisite 93A were selected for further investigation using *in situ* polymerization here. This selection is based on a balance between swelling behavior and type of solvent suitable for propylene polymerizaiton.

Unfortunately the swelling behavior of such clays in liquid propylene was not studied here because of the lack of experimental apparatus.

4.2 Supercritical Conditions

A rationale somewhat similar to the one described by Manke *et al* [24] will be employed in this work, although the other authors worked with supercritical CO_2 and prepared nanocomposites with extrusion. The process used here consists of swelling the clay in supercritical propylene followed by catastrophical depressurization into the polymerization reactor autoclave, where the *in situ* polymerization of PP is carried out using a supported Ziegler Natta catalyst.

One of the important characteristics of supercritical fluids is the capacity to tweak the solubility of a solute by changing the temperature and pressure. The effect of temperature and pressure for pre-treatment of clays in propylene above its critical point, and the effect of this pre-treatment on the properties of the nanocomposites were investigated in this work. In order to determine the limits of conditions that can be performed safely, pre-trials were done on the pressure vessel. The vessel was loaded with different amounts of propylene and the temperature was raised very slowly. The increase in pressure was monitored and the results are presented in Figure 19.

Figure 19 shows that at least 11.2g of propylene are needed in the pressure vessel order to achieve supercritical conditions. With such a small amount of propylene, it is possible to achieve supercritical pressure at temperatures higher than 200ºC. When the pressure vessel was almost full of liquid propylene (56g), the pressure increased

very rapidly with small increases in the temperature. Under this condition of vessel loading, the pressure at supercritical temperature achieved 3.500PSI.

One goal of this experiment was to investigate the conditions and the behavior of the apparatus in supercritical conditions, which is beyond the critical point (91ºC and 660psi). In conclusion, Figure 19 shows several conditions where supercritical conditions can be obtained. For example, with approximately 39.2g of propylene inside the pressure vessel it is easily possible to reach the critical point and work over a wide range of pressures and temperature within the supercritical range.

Note that some of the pressures used in these experiments are relatively high (at almost 6,500psi) and the proper type of material and components should be select to assemble such pressure vessel system to assure safety.
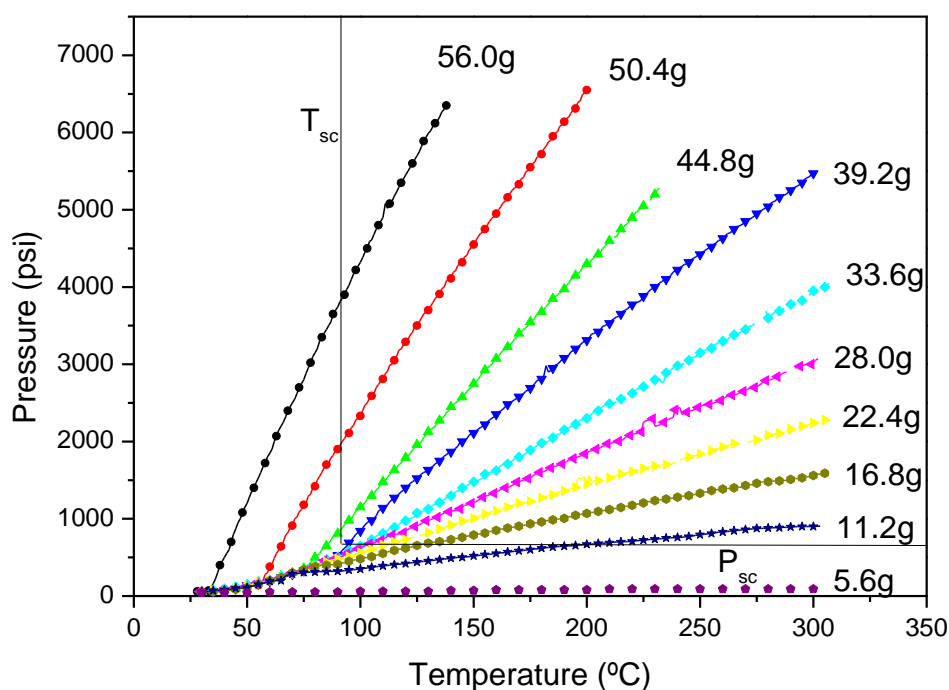
Figure 19. Pressure versus temperature at different propylene loadings in the pressure vessel.

4.3 *In situ* Polymerization

In this section, *in situ* polymerization of propylene and MMT without (4.3.1) and with (4.3.2) the use of supercritical fluid pre-treatment of the clay is presented and discussed.

The first part evaluates the effect of two organically modified clays on the properties of PP/MMT nanocomposites obtained via *in situ* polymerization. The *in situ* polymerization process used was previously described in the literature review. It involves the swelling of clay in a proper solvent followed by the addition of a supported Ziegler Natta catalyst and the polymerization of propylene using the slurry process [17].

The second part evaluated the effect of the clay pre-treatment <u>with</u> supercritical propylene followed by catastrophic depressurization of the clay into the polymerization reactor.

The following parameters were studied:

- catalyst performance
- structure of the polymer molecules
- polymer particle morphology
- dispersion of the clay.

4.3.1 *In situ* Polymerization without Supercritical Fluid Pre-Treatment

In a previous study, Dal Castel used supported Ziegler Natta catalyst to obtain PP/MMT nanocomposites using *in situ* polymerization [17]. It was showed that nanocomposites obtained using this method presented better clay dispersion when compared to nanocomposites with the same composition obtained by melt compounding. However, the lack of external donors during the polymerization resulted in PP with low isotactic index and, consequently, poor mechanical properties.

In order to create a baseline for further comparisons, polypropylene was synthesized using supported Ziegler Natta catalyst with the addition of external donor using conventional slurry process (solvent: toluene, cocatalyst with external donor: triethylaluminum (15mmol) and dicyclopentyldimetoxysilane (0.75mmol), catalyst (0.10mmol of Ti), temperature: 60ºC, propylene partial pressure: 70psi, reaction time: 1h.

The effect of adding two organically modified clays, previously swelled in toluene, to the polymerization reactor in order to obtain polypropylene/montmorillonite nanocomposites via *in situ* polymerization was also evaluated.

The performance of the catalyst was measured with productivity, that is the activity of the catalyst calculated based on the amount of polymer recovered at the end of the polymerization reaction (yield). The results are presented in Table 5. The

productivity of the catalyst in the polymerization without clay is used as a reference (Reaction PP on Table 5). The addition of the clay Cloisite 15A to the reactor strongly reduced the activity of the catalyst (Reaction C15A). As a consequence of the low productivity, a high clay loading was obtained in this nanocomposite. The clay Cloisite 93A, in its turn, promoted a small reduction in the catalyst activity, presenting a relative productivity of 94.6%.

Table 5. Catalyst activity and clay loading of the PP and nanocomposites prepared under normal conditions.

Reaction	Yield (gPP)	Productivity (kgPP/molTi)	Relative productivity (%)	Clay loading* (%)
PP	50.7	507.4	100.0	0
C15A	4.2	42.0	8.3	32.3
C93A	48.0	480.0	94.6	3.4

0.10mmol Ti; 15.0mmol Al, 60°C; 70psi, 1 hour.
*measured by TGA.

The causes for reduced activity in the presence of the clay are not fully understood. Some authors suggested that adsorbed water in the clay could be responsible for the reduction in the catalyst activity [115]. However, the Cloisite 15A is less hydrophilic than Cloisite 93A and should have a lower amount of adsorbed water, and consequently should present smaller reduction in activity. Another possible explanation is related to the fact that the cocatalyst can react with the modifier of the clay. In fact, Lee and coworkers [116] observed that more than 90% of the modifier was removed after the clay Cloisite 25A was treated with alkylaluminium. So, when the clay is swelled by the solvent the clay platelets are pushed apart from each other, exposing the organic modifier to react with the cocatalyst. This reaction consumes the cocatalyst making it unavailable for the catalyst. As shown previously, Cloisite 15A has more organic modifier and swells more easily in toluene than Cloisite 93A thus increasing the probability of consuming the cocatalyst. Therefore, it is plausible to consider that the organic modifiers present on the clay or the polar groups belonging to the natural structure of the clay are responsible for decreasing the catalyst activity and the reactor productivity.

The structure of the polymer molecules was investigated with FTIR. The isotacticity of the polypropylene was measured by FTIR according to methodology developed by Burfield *et al.* [117]. In this method, the absorbance of the band 998cm^{-1}, linked with isotactic polypropylene helixes containing 11-12 units, is normalized by the band 973 cm^{-1}, which corresponds to head-to-tail propylene units being also observed in molten iPP samples and completely atactic PP. The FTIR spectrum of PP obtained without the addition of clay is presented in Figure 20. The isotacticity index (II) was calculated using the following equation.

$$\text{Isotacticity Index } (\%) = \frac{abs_{998}}{abs_{973}} \, x \, \frac{1}{1,08} + 0,15$$

The isotacticity index calculated for the pure PP was 0.983±0.060. This result indicates good structural regularity in the polypropylene chains. Other indications of the high isotacticity index of the polypropylene chains are the high melting temperature, around 165°C, and crystallinity, around 45%, as presented in Table 6. These results are similar to the properties found in commercial grades of iPP [118, 119].
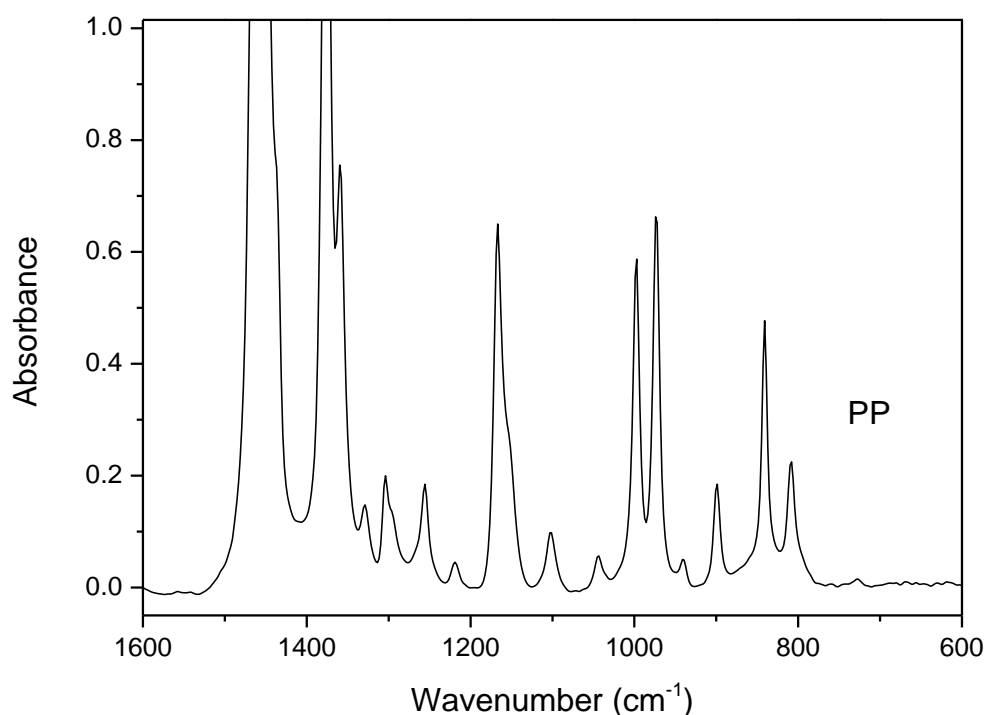
Figure 20. FTIR spectrum of PP without the addition of clay.

Table 6. Thermal properties of PP and PP/MMT nanocomposites

Reaction	T_c (ºC)	T_m (ºC)	ΔH_m (J/g)	Cristallinity (%)
PP	116	164	93.6	45.2
C15A	121	165	62.8	44.8
C93A	121	166	98.1	49.0

However it is not possible to measure the isotacticity index of the nanocomposites using the Burfield methodology, because the clay absorbs strongly in the range from 800 to 1300 cm^{-1}. Nonetheless, the melting temperature and crystallinity presented by the nanocomposites samples (C15A and C93A) indicated these materials also show high isotacticity.

The nanocomposites showed crystallization temperatures slightly higher than the pure polymer indicating that the clay acted as a nucleation agent. This effect is often observed in polymer/montmorillonite nanocomposites [45].

The growth of polymer particles formed during the polymerization of polyolefins using supported catalyst (type Ziegler-Natta) is usually described using the multigrain model. According to this model, the particle morphology evolution involves two steps: fragmentation and growth. Supported catalyst are particles highly porous with diameters typically ranging from 10-100μm. These catalyst particles are formed by smaller fragments called microparticles. During the polymerization process, these microparticles undergo a process of fragmentation due to the formation of polymer in their surface, and the structure, or morphology, of the particle begins to evolve. Depending on the polymerization conditions, the polymer particles formed can reach between 100 and 5000 μm in diameter, as shown in Figure 21 [120]. From an industrial point of view, it is highly desirable that the polymer particle presents a controlled morphology (preferably spherical) to avoid reactor fouling, thus making it easier to transport the product (higher bulk density) and to save energy during the incorporation of additives.

t = 0   t = 0⁺

+ monomer

catalyst particle (10-100 μm)

[agglomeration of smaller fragments
(microparticles), 0.001-0.5 μm]

polymer particle
(100-5000 μm)
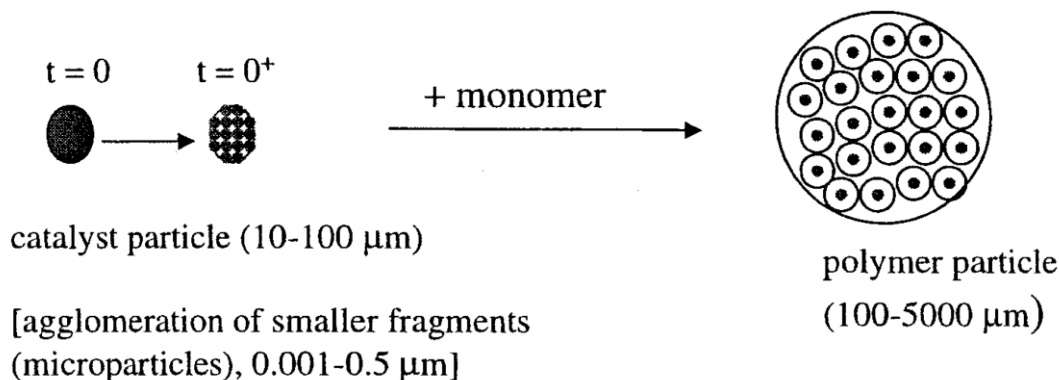
Figure 21. Schematic of polymer growth in polyolefin synthesis [120].

Figure 22 presents images of the polymer particles of pure PP and the nanocomposites with Cloisite 15A and Cloisite 93A. It is possible to see in the SEM images that the pure PP has good particle morphology with polymer particles with approximately 50μm in diameter. The inset image presents higher magnification where it is possible to see that the polymer particle is in fact formed by smaller microparticles as previously discussed.

The nanocomposites lost the controlled morphology of the catalyst, presenting polymer particles with irregular shapes and very broad size distribution although the microparticles are still visible at higher magnifications. As pointed out by Soares and McKenna, it is not always easy to control the fragmentation under full reactor conditions. Several parameters can promote an uneven fragmentation and loss of control over the morphology, such as particle overheating, high reaction rates, atactic PP, and low molecular weight.

In order to study the morphology of the polymer particle in the presence of clay, polymer particles obtained at the end of the polymerization were embedded in epoxy resin and ultrathin cuts (70-100nm) were imaged in a transmission electron microscope. Figure 23 shows a TEM image of a section of a polymer particle embedded in epoxy. In this figure, it is possible to see that the clay is located in the surface of the microparticles (inset) and that the polymer particle is formed by the agglomeration of polymer microparticles. This structure indicates that the microparticles fragmented during the polymerization and morphology of the catalyst was lost. At the end of the polymerization the polymer and clay were precipitated forming a polymer particle with irregular shape, as observed previously using SEM.
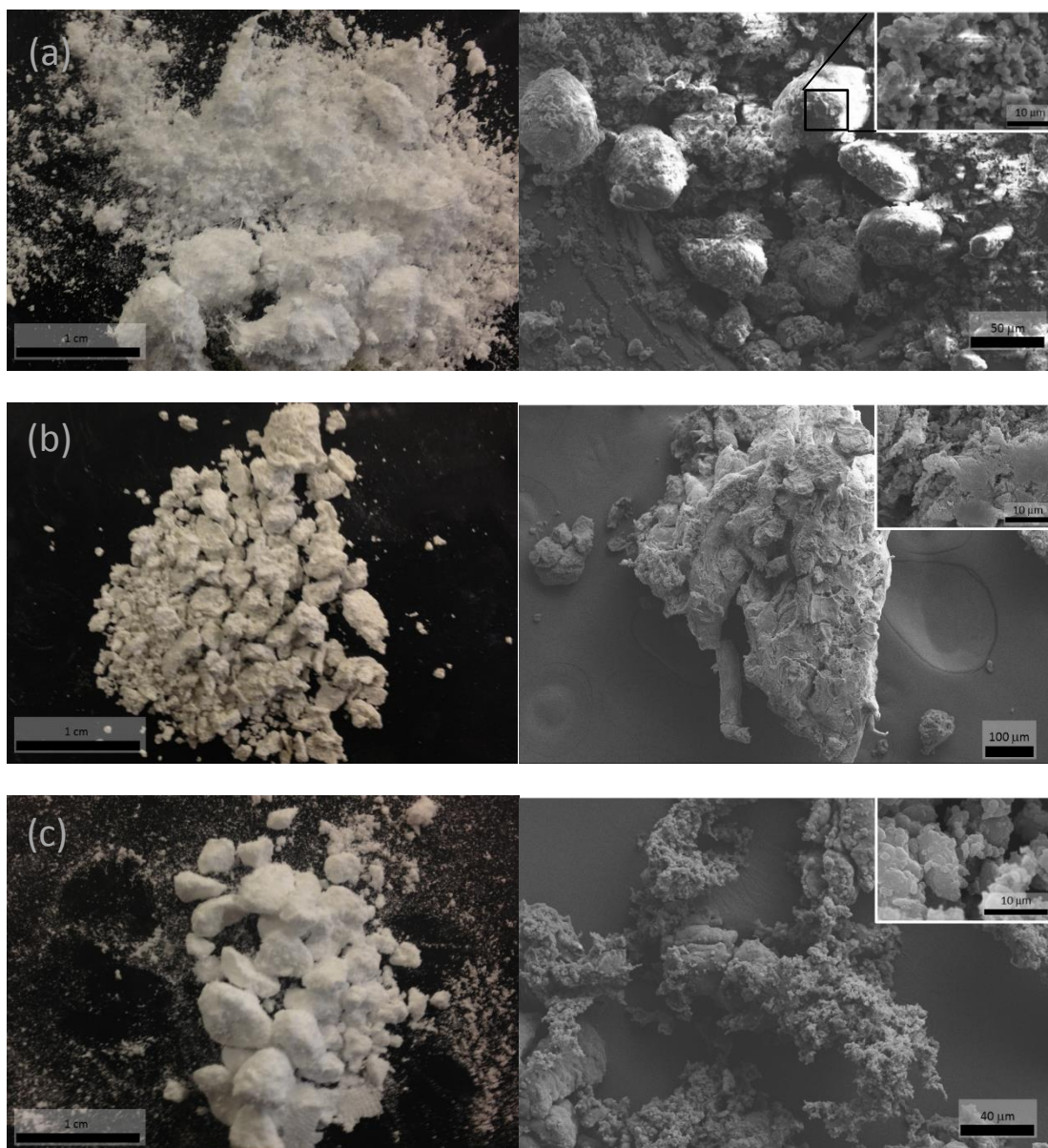
Figure 22. Pictures (left) and respective SEM images (right) of polymer particles obtained by *in situ* polymerization without addition of SCF: (a) PP, (b) C15A, (c) C93A.
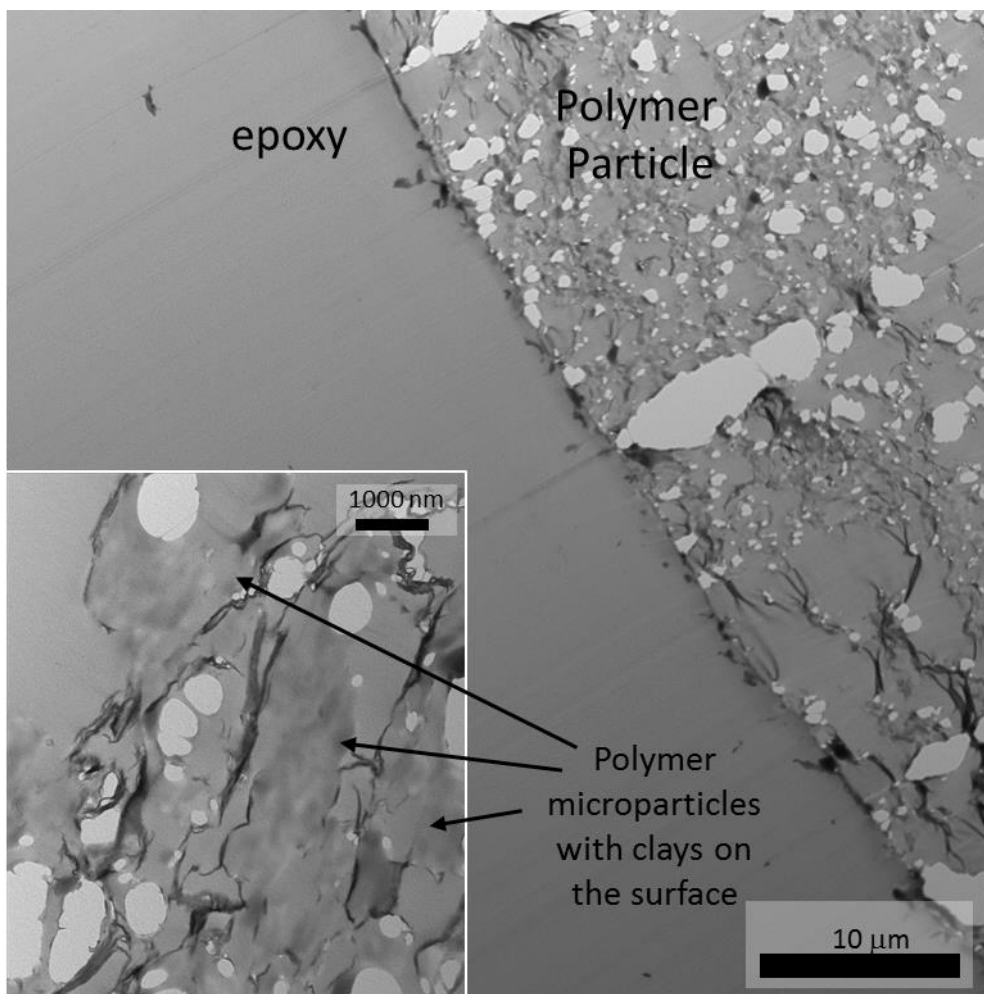
Figure 23. TEM image of the transversal section of a polymer particle of the C15A nanocomposite embedded in epoxy resin.

The dispersion and structure of the clay in the nanocomposites was further evaluated using XRD and TEM using samples that were prepared injection molding the product of the polymerization. The XRD patterns of the clays and the respective nanocomposites are presented in Figure 24. The peak corresponding to the 001 plane was used to calculate the interlamellar distance using the Bragg's law. Based in these results it is possible to see that there is clay that was not intercalated by the polypropylene chains. In fact, both clays presented peaks shifted to higher angles, corresponding to a decrease of approximately 1nm in d_{001}. This result reinforces the idea that the cocatalyst may have reacted with the organic modifier of the clay, washing it out of the clay galleries, and consequently reducing the interlamellar d_{001}.
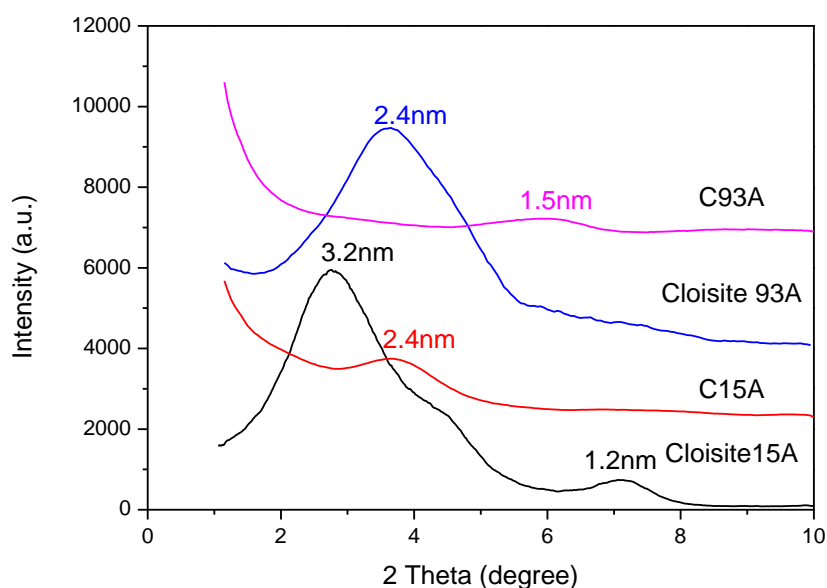
Figure 24. XRD patterns of the modified montmorillonite and nanocomposites prepared by *in situ* polymerization without SCF pre-treatment.

The dispersion level of the clays in the nanocomposites obtained by *in situ* polymerization was studied by TEM and the results are presented in Figure 25. The PP/MMT nanocomposites prepared with Cloisite 15A presented agglomerates around 2-5μm long and 0.5-1.0μm thick with hardly any signs of exfoliation. The nanocomposite prepared with Cloisite 93A, in turn, presented better dispersion, with agglomerates around 0.5-2μm long and 0.1-0.2 μm thick. Although the Cloisite 15A presents a more hydrophobic characteristic than the Cloisite 93A, which would suggest a better interaction with polypropylene, it is necessary to consider that the nanocomposite C15A has a much higher clay loading and this could explain the reduced dispersion of the montmorillonite in this nanocomposite.

These results indicate that the Cloisite 93A is the most appropriate clay in obtaining PP/MMT nanocomposites via *in situ* polymerization (without using supercritical fluid) due to the combination of good dispersion of the clay and good catalytic activity. Thus this clay will be used in the next section to prepare nanocomposites using supercritical propylene.
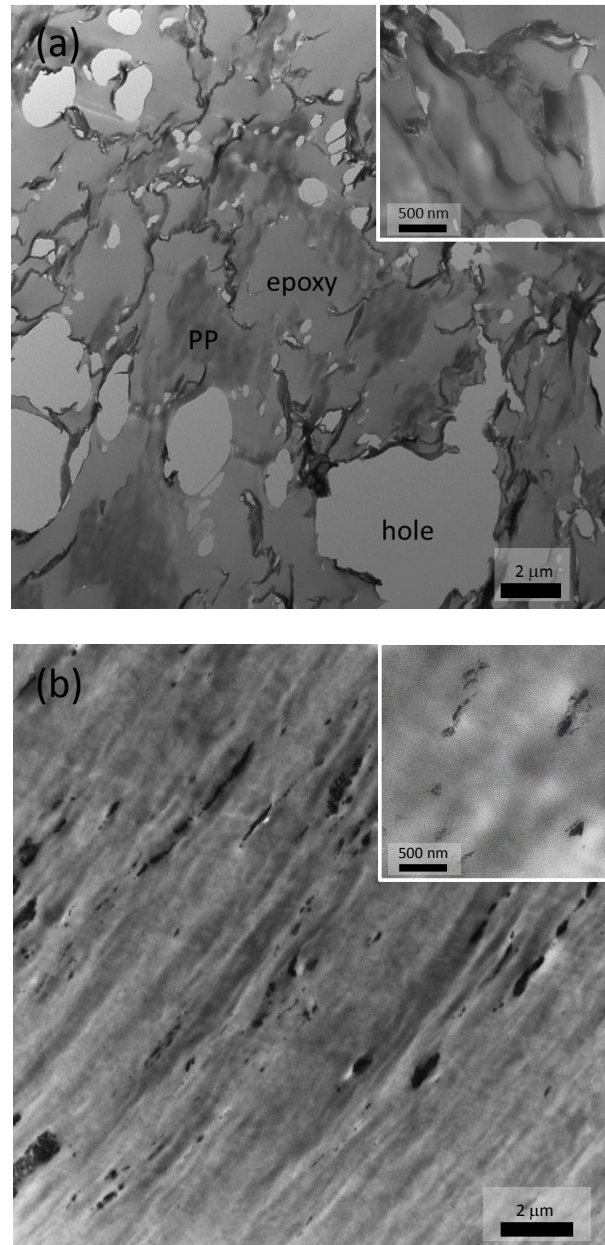
Figure 25. TEM images of the particles of PP/MMT nanocomposites embedded in epoxy resin: (a) C15A, (b) C93A.

4.3.2 *In situ* Polymerization with Supercritical Fluid Pre-Treatment

In this section the effect of pre-treatment of the clay in four different supercritical conditions on the properties of PP/MMT nanocomposites is discussed. Table 7 presents these supercritical conditions used in the pre-treatment of the clay. Four supercritical conditions were selected, each condition is indicated with a point on Figure 26:

- point 1 is slightly above the critical point

- point 2 is close to the critical temperature with pressure well above the critical point

- point 3 has both pressure and temperature well above the critical point

- point 4 is near the maximum pressure and temperature limit of pressure vessel used for this experiment

Additionally, Figure 26 and Figure 27 show the conditions of pressure and temperature used in the pre-treatment of clay before and after catastrophic decompression in the reactor. The initial points are clearly defined since the pressure vessel has good control of temperature and pressure. The final conditions are given as a range due to the temperature lag in the reactor autoclave. The actual path in the phase diagram that the mixture of supercritical propylene and Cloisite 93A took during the decompression towards the reactor is not known at this time and it was not part of the scope of the research present here to determine it.

Table 7. Supercritical conditions used for the pre-treatment of the clay prior to *in situ* polymerization.

Condition	Temperature[1] (ºC)	Pressure[1] (psi)	Density[2] (kg/m^3)
PP*	92	700	230
1	92	700	230
2	125	5500	471
3	190	5000	400
4	200	5750	410

* without clay.
[1] in the pressure vessel.
[2] Supercritial propylene density obtained from diagram.

The catalyst activity of PP produced by the conventional method and the PP produced by the addition of supercritical propylene are presented in Table 8. The results show that the simple addition of supercritical propylene does not affect the productivity of the catalyst with both reactions (PP and PP*) producing similar yield.
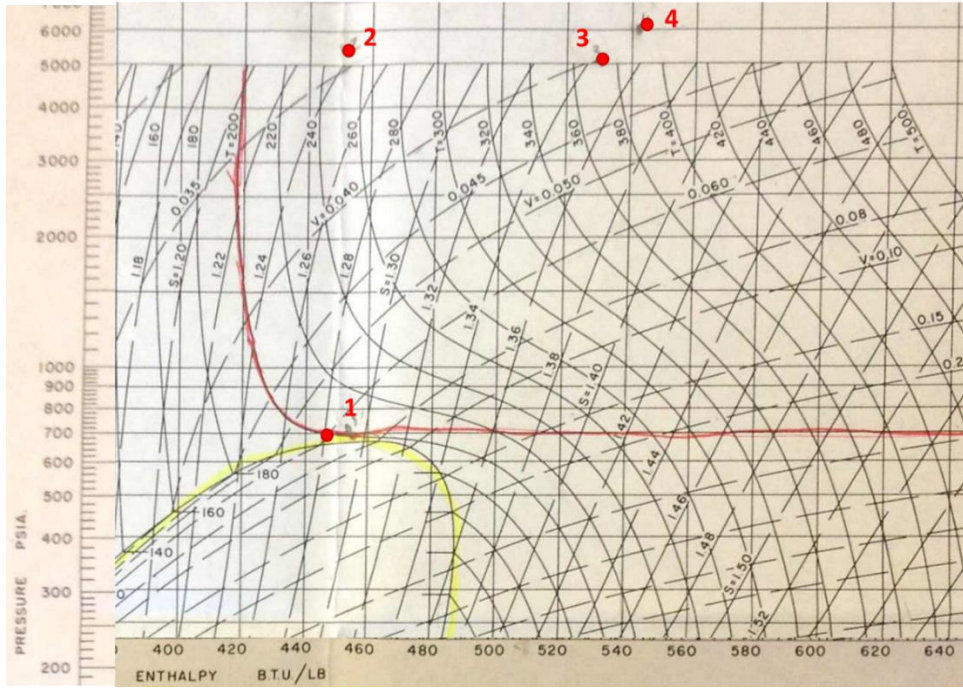
Figure 26. Conditions of pressure and temperature used in the pre-treatment of clay before catastrophic decompression in the reactor.
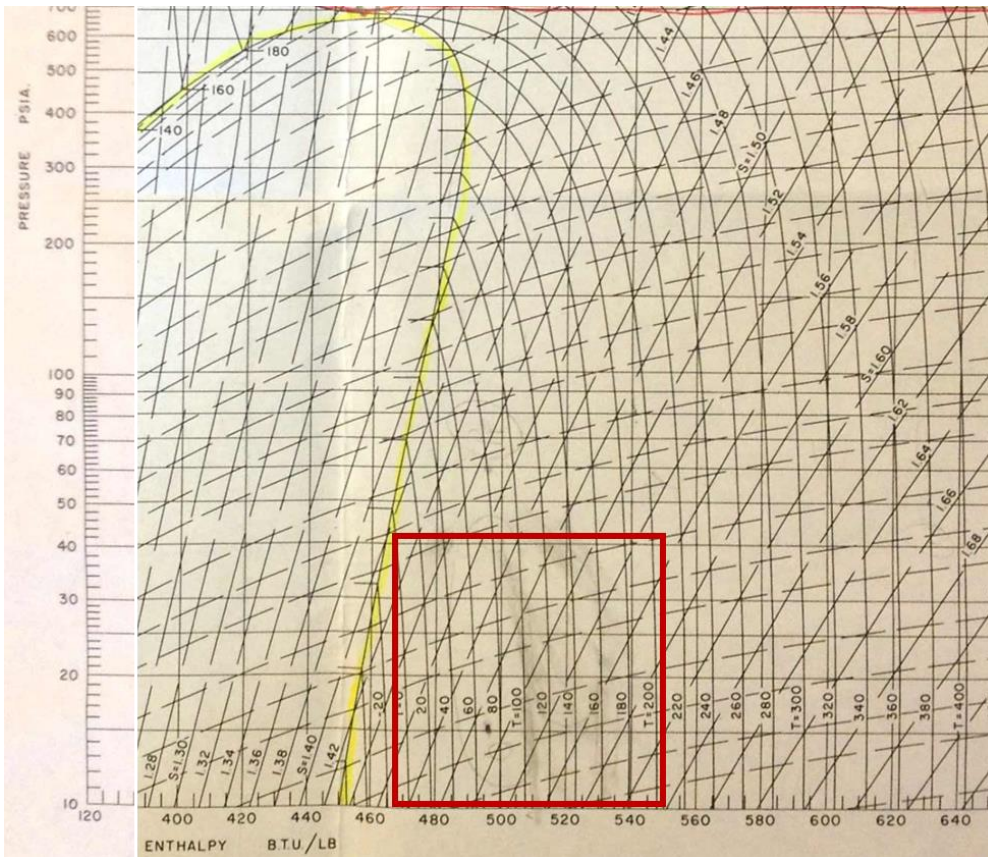
Figure 27. Expected range of pressure and temperature after catastrophic decompression of the clay in the reactor.

Table 8 lists the polymerization reactions loading clay treated with supercritical propylene (Reactions 1-4), the polymerization reaction with Cloisite 93A without treatment with supercritical propylene (Reaction C93A), the polymerization reaction loaded with supercritical propylene without clay (Reaction PP*), as well as the polymerization reaction without Cloisite 93A and supercritical propylene (Reaction P, same entry in Table 5 is added to Table 8 to facilitate comparison).

Table 8. Catalyst activity and clay loading of the PP and nanocomposites prepared with Cloisite 93A under supercritical conditions.

Reaction	Yield (gPP)	Productivity (kgPP/molTi)	Relative productivity (%)	Clay loading[1] (%)
PP	50.7	507.4	100.0	0
C93A	48.0	480.0	94.6	3.4
PP*	50.3	503.0	99.1	0
1	27.9	279.0	55.0	4.7
2	30.0	300.0	59.1	3.8
3	31.0	310.0	61.1	3.5
4	15.2	152.0	30.0	6.7

0.10mmol Ti; 15.0mmol Al, 60°C; 70psi, 1 hour.
* without clay.
[1]measured by TGA.

Adding the clay treated with supercritical propylene to the autoclave reactor using the decompression affected the productivity of the catalyst. The productivity of the catalyst was reduced to approximately 60% for Reactions 1-3 (using supercritical propylene at points 1-3) when compared to Reaction PP.

Reaction 4 (using supercritical propylene at point 4) presented productivity of only 30% compared to Reaction PP. These results are lower than adding clay without the supercritical pre-treatment as shown in Table 5. One possible explanation is that the supercritical pre-treatment is promoting better exfoliating of the clay exposing more of this surface, with in turn can react with the cocatalyst as discussed in the previous session. The Reaction 4 used clay treated with supercritical propylene at the highest pressure and temperature (200°C), which may have also contributed to change the

chemical composition at the surface of Cloisite 93A by extracting the quaternary ammonium salt. Reports in the literature have shown that Cloisite 93A has a thermal stability above 200°C [43]. But the in the supercritical propylene the high diffusivity of the supercritical fluid may have contributed to removal of the quaternary ammonium salt. At the present moment there are no information to provide a definite explanation for the decrease in activity.

Another reason for the reduced catalytic activity could be the reduced transport of propylene towards the catalyst particle due to the presence of the clay on the surface of the polymer particle forming a barrier to the diffusion of propylene. Other reports in the literature [12] have concluded that distribution of clay at the nanoscale within a polymer matrix can reduce permeability to gases.

Figure 28 shows the FTIR spectrum of polypropylene obtained with (PP*) and without (PP) addition of supercritical propylene. Again, using the Burfield *et al. [117]* method, it was possible to determine the isotacticy index (II) of the PP molecules. The II for the polypropylene produced with addition of SCF, PP*, was 1.02±0.06, compared with 0.98±0.06 for the PP. This indicates that the addition of SCF does not affect the tacticity of the resulted product.
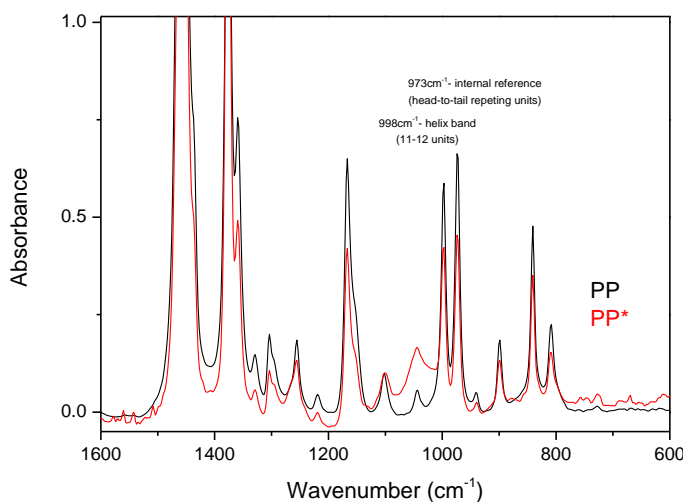
Figure 28. FTIR spectrum of polypropylene obtained with (PP*) and without (PP) addition of SCF.

As previously discussed, the II of the nanocomposites cannot be measured by FTIR, however the high melting temperature and crystallinity presented in all nanocomposites, as shown in Table 9, indicate high isotacticity of the polypropylene

chains. Once again, the nanocomposites showed crystallization temperatures slightly higher than the pure polymer indicating that the clay acted as a nucleation agent.

The morphology of the polymer particles obtained from the autoclave reactor can be discussed at three levels of hierarchy:

- Powder or aggregates: Visible to the naked eye, it is formed by a growth of polymer around a single catalyst or by agglomeration of those polymer particles. Its structure is highly dependable in the reactor conditions such as temperature, type of solvent, filtration and drying.

- Polymer particle: Formed by the fragmentation and growth of microparticles of the catalyst staying together. The individual polymer particles can be 10 to 1,000 times bigger than the original catalyst particle. The size and shape of the individual polymer particles depends on the reaction rate, fragmentation mechanism and characteristics of polymer formed around the catalyst support (solubility of polymer chains, modulus and strength of polymer) It also replicates the shape of the catalyst particle.

- Microparticle. This morphology deals with the smallest particles formed around the individual catalyst active sites.

Table 9. Thermal properties of PP and PP/MMT nanocomposites

Reaction	T_c (°C)	T_m (°C)	ΔH_m (J/g)	Crystallinity (%)
PP	116	164	93.6	45.2
C93A	121	166	98.1	49.0
PP*	117	164	93.6	49.5
1	122	166	101.0	51.2
2	124	165	85.3	42.8
3	121	166	100.2	50.1
4	124	164	81.4	42.3

0.10mmol Ti; 15.0mmol Al, 60°C; 70psi, 1 hour.
* without clay.

In Figure 29, it is possible to observe these three levels of hierarchy. In the inset of the SEM images, it is possible to see the microparticles of polymer. They present globular structures with approximately 1μm in diameter in both PP and PP*. The polymer particles were also very similar for these two samples, presenting spherical shape with size around 50μm. The results indicate that in the polymerization conditions allowed the catalyst to maintain its morphology which is very desirable for industrial applications.
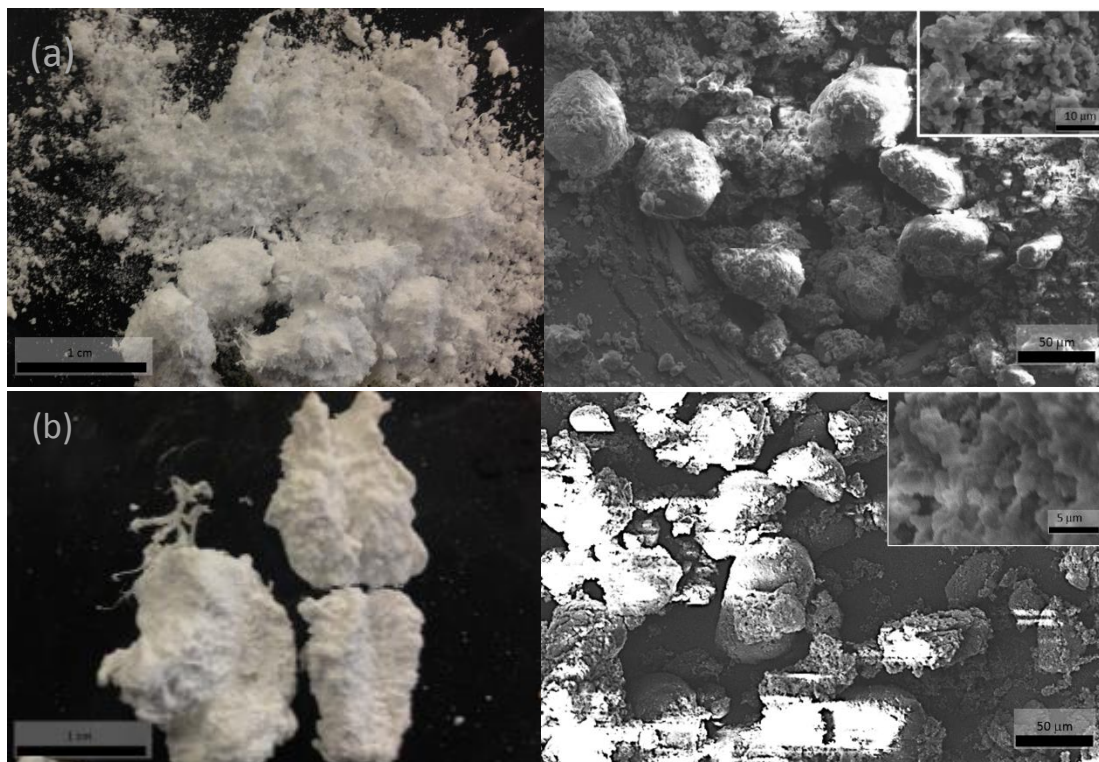
Figure 29. Photographs (left) and respective SEM images (right) of polymer particles of PP obtained by without (PP (a)) and with (PP* (b)) the addition of SCF.

The images on the left side of Figure 29 show the powder structure for PP and PP*. As seen previously, their microstructures are very similar, however their powder structures appear very different, with the PP showing a fine powder while PP* displaying large agglomerates. This is a result of their processing and history associated to recover the product from the reactor, with PP* agglomerates being formed during filtration.

The morphology of the nanocomposites obtained by *in situ* polymerization with addition of supercritical propylene are presented in Figure 30. The addition of clay and its exfoliation mechanism adds another level of complexity to the mechanism of

polymer particle growth. It is possible to see that the microparticles morphology is still present in the polymer particles, indicating that the polymer was not solubilized during the polymerization in none of the samples. This is expected because the measurement of crystallinity indicated that the polypropylene is capable of crystallizing in the solid state. Therefore it is concluded that the solubility of polypropylene chains being formed during the polymerization were not affected by the addition of clay treated with supercritical propylene.

Although no change was observed in the microparticle structure, a significant modification was observed in both the polymer particle and powder structure of the nanocomposites when compared with pure PP. This could be attributed to an uneven fragmentation of the catalyst promoted by the clay and consequently the loss of control of the morphology of the polymer particle. The polymer particles in the nanocomposites present irregular shape with sizes several times bigger than those in the pure PP.

Uneven fragmentation of the catalyst should produce smaller particles; however the precipitation of clay in the surface of these particles is, somehow, keeping them together. The Figure 23 supports this supposition.

The dispersion of the clay in the nanocomposites prepared with SCF pre-treatment was evaluated using XRD and TEM. The XRD patterns of the clay and the nanocomposites prepared with different supercritical conditions are presented in Figure 31. It is not possible to see the diffraction peak in the sample 1, what could indicate a complete exfoliation of the clay. Sample 2 did not present any shift in the peak position indicating no variation in the interlamellar distance. However, sample 3 and 4 presented peak shifted to higher angles, corresponding to a decrease in d_{001} of approximately 0.5 and 0.7nm, respectively. This reduction could be ascribed to the degradation or extraction of the quaternary ammonium salt by high temperature or, as mentioned before, to its reaction with the cocatalyst.

The dispersion level of the clay in the nanocomposites obtained by *in situ* polymerization with and without SCF pre-treatment are presented in Figure 32. The nanocomposites prepared using supercritical pre-treatment clearly displayed higher exfoliation level than the sample prepared without SCF pre-treatment. The exfoliation is observed because relatively thin particles were obtained. In regard to the samples prepared with SCF, there is no clear trend relating the supercritical conditions with the exfoliation level. Samples 1 and 3 presented very high exfoliation levels with clay particles ranging from 10 to 30 nm thick and 100 to 700nm long.

54
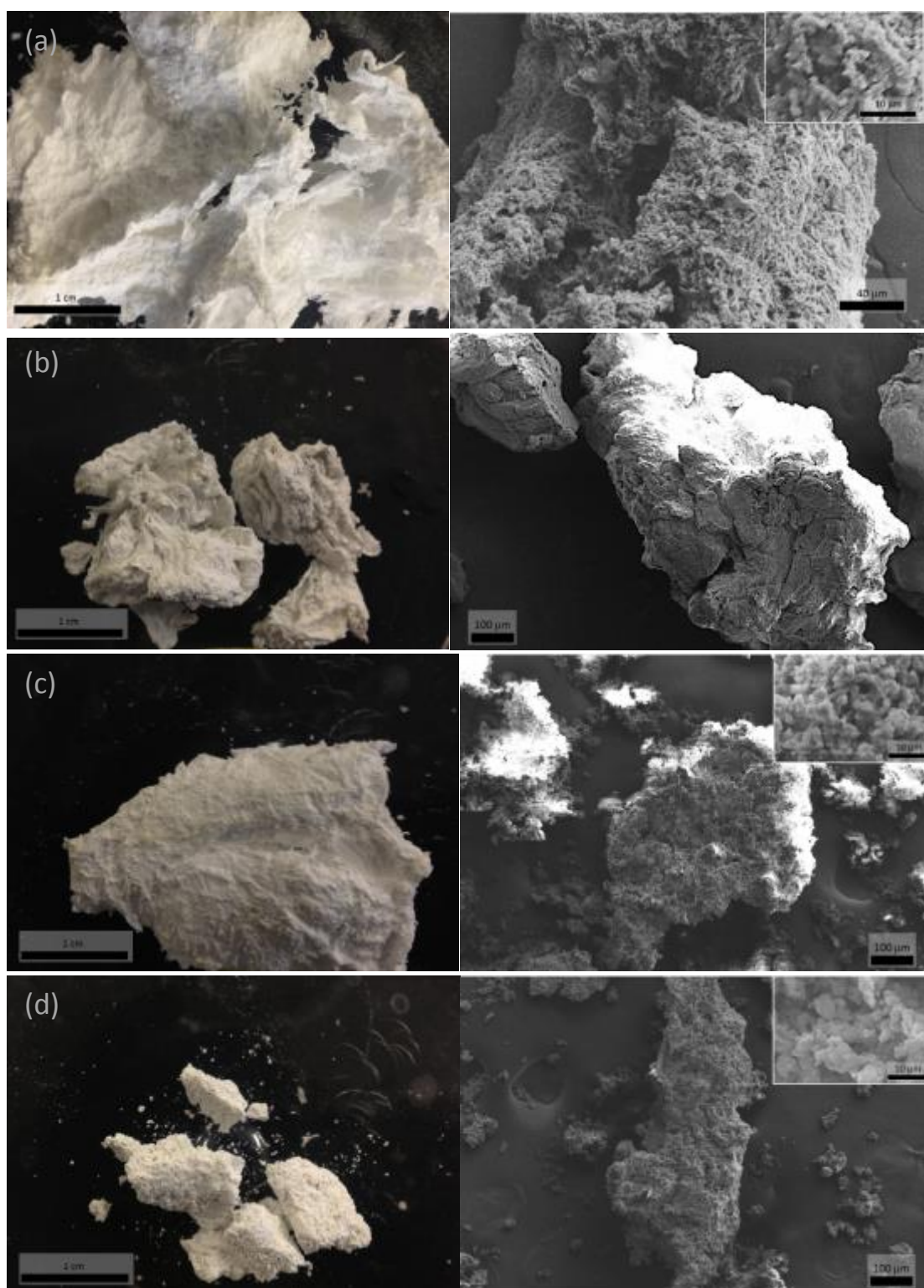
Figure 30. Photographs (left) and respective SEM images (right) of polymer particles obtained by *in situ* polymerization with addition of SCF. Reactions: (a) 1, (b) 2, (c) 3, (d) 4.
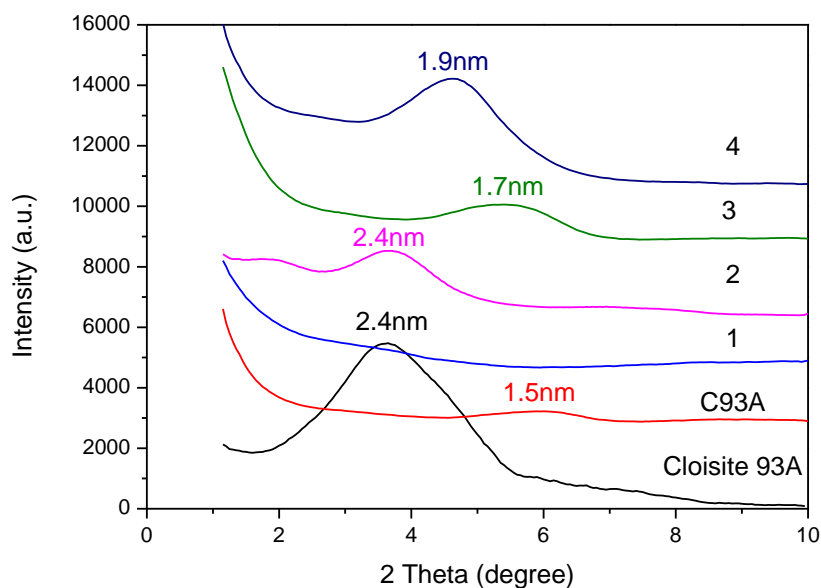
Figure 31. XRD patterns of the modified montmorillonite and nanocomposites prepared by *in situ* polymerization without (C93A) and with SCF pre-treatment (1-4).

Although samples 2 and 4 presented better clay dispersion than sample prepared without SC propylene (C93A), the clay dispersion was lower than samples 1 and 3. Samples 2 and 4 showed clay particle size with width around 100 to 200nm and length around 600 to 2000nm.
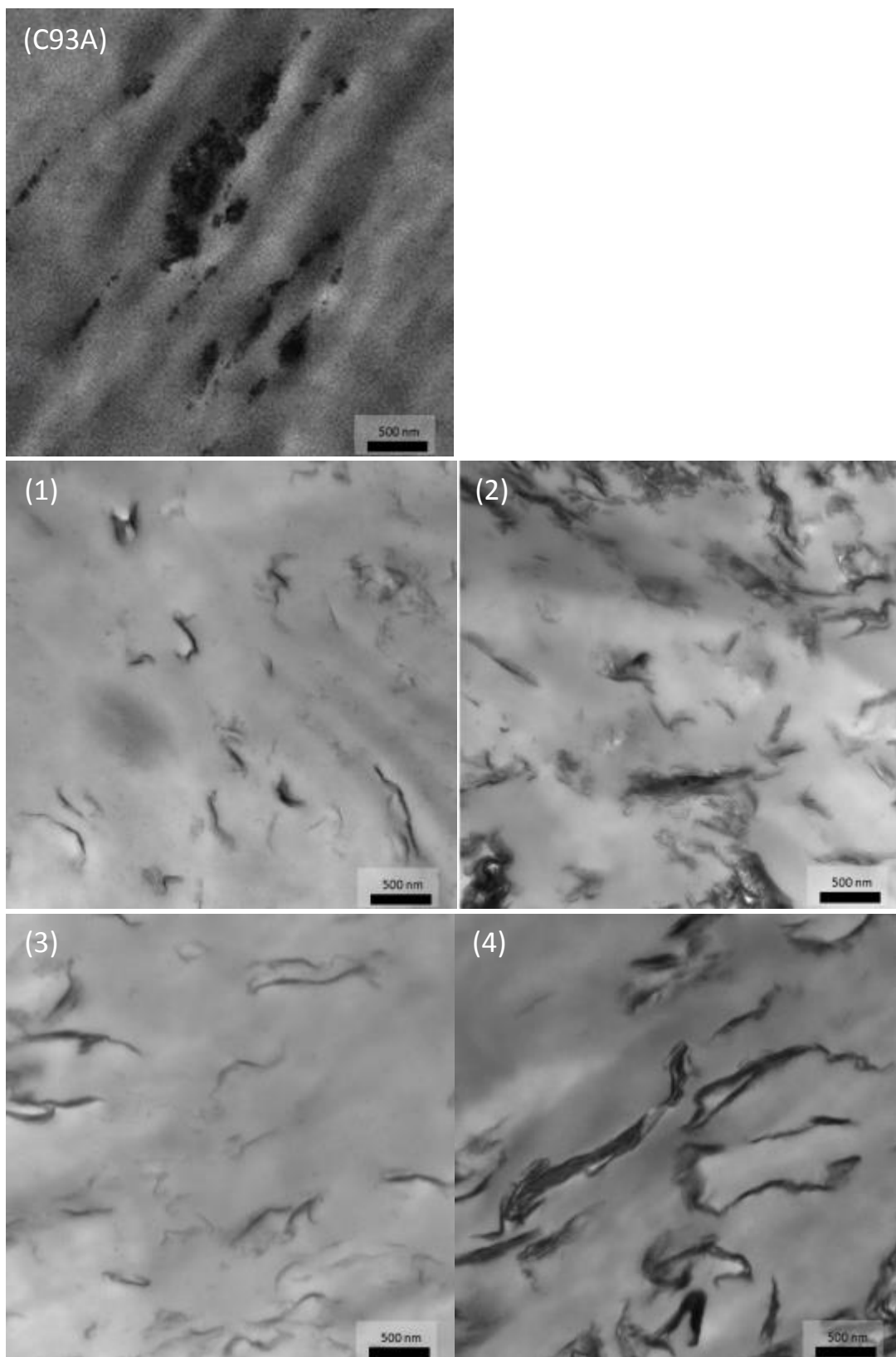
Figure 32. TEM images of PP/MMT nanocomposites prepared by *in situ* polymerization with Cloisite 93A polymerization without supercritical propylene (sample C93A) and with Cloisite 93 using supercritical propylene treatment (samples 1-4, corresponding to Reactions 1-4 in Table 8).

57

5 CONCLUSIONS AND RECOMMENDATIONS

5.1 Conclusions

It is well established in the literature that the exfoliation of the clay strongly improve the properties of polymer/montmorillonite nanocomposites. In this work, the use of supercritical propylene to produce polypropylene/clay nanocomposites via *in situ* polymerization was studied.

The results showed that it is necessary to optimize a series of parameters in order to achieve high levels of exfoliation of the clay in the PP matrix. The main points are presented below.

Choice of solvent and clay: Montmorillonite has a strong polar character, which is reduced when the clay is modified by ammonium quaternary salts with long alkyl chains. However this clay still presents limited compatibility of solvents with very low relative polarity such as hexane and cyclohexane (Table 4). Thus a solvent with higher polarity should be used in order to disperse the clay. However, Ziegler –Natta catalyst are very sensitive to polar solvents limiting the number of solvents that can be used during polymerization. The best solvent in this case should be a hydrocarbon with relatively high polarity, such as toluene. The clay modifier must promote good dispersion in the solvent and promote no or little reduction in the catalyst activity. Cloisite 93A was the clay that presented the best properties among the ones tested in this work.

Solvent-clay mixing conditions: The results showed that mixing condition presents an important parameter affecting the clay dispersion in the solvent. The use of a sonication bath was much more effective in swelling the clay than manual mixing. It was assumed that the supercritical propylene would swell the clay quickly due to its high diffusion coefficient; however further testing is needed to confirm it.

Catalyst Performance: The addition of clay to the polymerization reactor reduces the productivity of the catalyst. The causes of this reduction are not completely understood but they can be related to consumption of cocatalyst or formation of a diffusion barrier to the transport of monomer. An interesting aspect of the catalyst performance was the high isotacticity of the polymer molecules which is crucial for obtaining polypropylene with good mechanical properties.

The addition of clay also led to the loss of control of the polymer particle morphology. This problem is a serious restriction to the application of this method in an industrial application and it should be further studied.

Clay pre-treatment: Although the addition of the clay promoted a reduction of the catalyst performance, the pre-treatment of the clay with supercritical propylene strongly improved the exfoliation level of the clay in the PP matrix when compared with PP/MMT nancomposites prepared by *in situ* polymerization without the pre-treatment of the clay with supercritical propylene.

5.2 Recommendations for Future Works

Although good exfoliation results were obtained in this work, the author suggests that the following evaluations should be carried out in order to better understand the polymerization and exfoliation mechanism and their results in the PP/MMT nanocomposites properties.

- Improve the mechanism to force the propylene molecules inside the clay galleries by adding mechanical agitation or even sonication in the high pressure vessel with propylene at supercritical state.

- Design an apparatus with a sapphire window in order to observe the behavior of clay swelling in different supercritical conditions such as: pressure, temperature agitation and time.

- Evaluate the clay degradation due to the effect of time, temperature and pressure under supercritical conditions. FTIR, TGA and X-ray are simple techniques that might be used to detect it.

- Evaluate the interaction between the ammonium quaternary salt used to modify the clay and the cocatalyst.

- Evaluate the influence of non-supported catalyst, such as metallocenes, on polymer production and clay dispersion.

- Carry out a polymerization in an gas-phase reactor.

- Evaluate the PP/MMT nanocomposites structure and properties such as: molecular weight, mechanical properties, thermal properties, barrier properties and flame retardancy properties.

- Evaluate other nanoparticles such as: graphite, nanocellulose, cabon nanotubes and silicon whiskers.

REFERENCES

1. Karian, HG, *Handbook of Polypropylene and Polypropylene Composites*. 2nd ed2003, New York: Marcel Deker.
2. Ray, SS, Okamoto, M, *Polymer/Layered Silicate Nanocomposites: A Review from Preparation to Processing.* Progress in Polymer Science, **2003**, 28(11), 1539-1641.
3. Usuki, A, Kojima, Y, Kawasumi, M, Okada, A, Fukushima, Y, Kurauchi, T, Kamigaito, O, *Synthesis of Nylon 6-Clay Hybrid.* Journal of Materials Research, **1993**, 8(5), 1179-1184.
4. Sanchez, C, Julian, B, Belleville, P, Popall, M, *Applications of Hybrid Organic-Inorganic Nanocomposites.* Journal of Materials Chemistry, **2005**, 15(35-36), 3559-3592.
5. Lagaly, G, *Smectitic Clays as Ionic Macromolecules*, in *Developments in Ionic Polymers—2*, Wilson A and Prosser, H, Editors. 1986 Springer Netherlands.
6. Reddy, CR, Sardashti, AP, Simon, LC, *Preparation and Characterization of Polypropylene-Wheat Straw-Clay Composites.* Composites Science and Technology, **2010**, 70(12), 1674-1680.
7. Furlan, LG, Ferreira, CI, Dal Castel, C, Santos, KS, Mello, ACE, Liberman, SA, Oviedo, MS, Mauler, RS, *Effect of Processing Conditions on the Mechanical and Thermal Properties of High-Impact Polypropylene Nanocomposites.* Materials Science and Engineering A Structural Materials Properties Microstructure and Processing, **2011**, 528(22-23), 6715-6718.
8. Kato, M, Usuki, A, Hasegawa, N, Okamoto, H, Kawasumi, M, *Development and Applications of Polyolefin- and Rubber-Clay Nanocomposites.* Polymer Journal, **2011**, 43(7), 583-593.
9. Spencer, MW, Hunter, DL, Knesek, BW, Paul, DR, *Morphology and Properties of Polypropylene Nanocomposites Based on a Silanized Organoclay.* Polymer, **2011**, 52(23), 5369-5377.
10. Dal Castel, C, Pelegrini Jr, T, Barbosa, RV, Liberman, SA, Mauler, RS, *Properties of Silane Grafted Polypropylene/Montmorillonite Nanocomposites.* Composites Part A: Applied Science and Manufacturing, **2010**, 41(2), 185-191.
11. Santos, KS, Liberman, SA, Oviedo, MaS, Mauler, RS, *Polyolefin-Based Nanocomposite: The Effect of Organoclay Modifier.* Journal of Polymer Science Part B-Polymer Physics, **2008**, 46(23), 2519-2531.
12. Giannakas, A, Spanos, CG, Kourkoumelis, N, Vaimakis, T, Ladavos, A, *Preparation, Characterization and Water Barrier Properties of PS/Organo-Montmorillonite Nanocomposites.* European Polymer Journal, **2008**, 44(12), 3915-3921.
13. Chiu, F-C, Chu, P-H, *Characterization of Solution-Mixed Polypropylene/Clay Nanocomposites without Compatibilizers.* Journal of Polymer Research, **2006**, 13(1), 73-78.
14. Filippi, S, Marazzato, C, Magagnini, P, Famulari, A, Arosio, P, Meille, SV, *Structure and Morphology of Hdpe-G-Ma/Organoclay Nanocomposites: Effects of the Preparation Procedures.* European Polymer Journal, **2008**, 44(4), 987-1002.
15. Choi, YY, Shin, SYA, Soares, JBP, *Preparation of Polyethylene/Montmorillonite Nanocomposites through in Situ Polymerization Using a Montmorillonite-Supported Nickel Diimine Catalyst.* Macromolecular Chemistry and Physics, **2010**, 211(9), 1026-1034.
16. Yang, K, Huang, Y, Dong, J-Y, *Efficient Preparation of Isotactic Polypropylene/Montmorillonite Nanocomposites by in Situ Polymerization Technique Via a Combined Use of Functional Surfactant and Metallocene Catalysis.* Polymer, **2007**, 48(21), 6254-6261.

17. Dal Castel, C, *Comparative Study of Polypropylene/Montmorillonite Nanocomposites Using Different Synthetic Routes*, 2012, Federal University of Rio Grande do Sul Porto Alegre, Brazil.
18. Zhao, Q, Samulski, ET, *In Situ Polymerization of Poly(Methyl Methacrylate)/Clay Nanocomposites in Supercritical Carbon Dioxide.* Macromolecules, **2005**, 38(19), 7967-7971.
19. Langat, J, Bellayer, S, Hudrlik, P, Hudrlik, A, Maupin, PH, Gilman Sr, JW, Raghavan, D, *Synthesis of Imidazolium Salts and Their Application in Epoxy Montmorillonite Nanocomposites.* Polymer, **2006**, 47(19), 6698-6709.
20. Urbanczyk, L, Ngoundjo, F, Alexandre, M, Jerome, C, Detrembleur, C, Calberg, C, *Synthesis of Polylactide/Clay Nanocomposites by in Situ Intercalative Polymerization in Supercritical Carbon Dioxide.* European Polymer Journal, **2009**, 45(3), 643-648.
21. Zhao, Q, Samulski, ET, *Supercritical CO2-Mediated Intercalation of PEOin Clay.* Macromolecules, **2003**, 36(19), 6967-6969.
22. Treece, MA, Oberhauser, JP, *Processing of Polypropylene-Clay Nanocomposites: Single-Screw Extrusion with in-Line Supercritical Carbon Dioxide Feed Versus Twin-Screw Extrusion.* Journal of Applied Polymer Science, **2007**, 103(2), 884-892.
23. Chen, C, Samaniuk, J, Baird, DG, Devoux, G, Zhang, M, Moore, RB, Quigley, JP, *The Preparation of Nano-Clay/Polypropylene Composite Materials with Improved Properties Using Supercritical Carbon Dioxide and a Sequential Mixing Technique.* Polymer, **2012**, 53(6), 1373-1382.
24. Manke, CW, Gulari, E, Mielewski, DF, Lee, EC, *System and Method of Delaminating a Layered Silicate Material by Supercritical Fluid Treatment*, 2000, Ford Global Technologies, Inc.
25. Callister Jr, WD, *Materials Science and Engineering* 7ª ed. ed2007, New York: Wiley.
26. Sandler, JKW, Kirk, JE, Kinloch, IA, Shaffer, MSP, Windle, AH, *Ultra-Low Electrical Percolation Threshold in Carbon-Nanotube-Epoxy Composites.* Polymer, **2003**, 44(19), 5893-5899.
27. Fornes, TD, Paul, DR, *Modeling Properties of Nylon 6/Clay Nanocomposites Using Composite Theories.* Polymer, **2003**, 44(17), 4993-5013.
28. Flandin, L, Prasse, T, Schueler, R, Schulte, K, Bauhofer, W, Cavaille, JY, *Anomalous Percolation Transition in Carbon-Black–Epoxy Composite Materials.* Physical Review B, **1999**, 59(22), 14349-14355.
29. Sazonova, V, Yaish, Y, Ustunel, H, Roundy, D, Arias, TA, Mceuen, PL, *A Tunable Carbon Nanotube Electromechanical Oscillator.* Nature, **2004**, 431(7006), 284-287.
30. Ajayan, PM, Schadler, LS, Braum, PV, *Nanocomposite Science and Technology*2003, Weinheim: Wiley.
31. Shenoy, MA, Patil, M, *Studies in Reduction of Molecular Weight of Polypropylene.* Polymer Science Series B, **2010**, 52(3-4), 174-183.
32. Dorigato, A, Pegoretti, A, *Fracture Behaviour of Linear Low Density Polyethylene – Fumed Silica Nanocomposites.* Engineering Fracture Mechanics, **2012**, 79(0), 213-224.
33. Naffakh, M, Díez-Pascual, AM, Marco, C, Ellis, GJ, Gómez-Fatou, MA, *Opportunities and Challenges in the Use of Inorganic Fullerene-Like Nanoparticles to Produce Advanced Polymer Nanocomposites.* Progress in Polymer Science, **2013**, 38(8), 1163-1231.
34. Kango, S, Kalia, S, Celli, A, Njuguna, J, Habibi, Y, Kumar, R, *Surface Modification of Inorganic Nanoparticles for Development of Organic–Inorganic Nanocomposites—a Review.* Progress in Polymer Science, **2013**, 38(8), 1232-1261.
35. Cho, M-J, Park, B-D, *Tensile and Thermal Properties of Nanocellulose-Reinforced Poly(Vinyl Alcohol) Nanocomposites.* Journal of Industrial and Engineering Chemistry, **2011**, 17(1), 36-40.
36. Rahmat, M, Hubert, P, *Carbon Nanotube–Polymer Interactions in Nanocomposites: A Review.* Composites Science and Technology, **2011**, 72(1), 72-84.

37. Lonjon, A, Caffrey, I, Carponcin, D, Dantras, E, Lacabanne, C, *High Electrically Conductive Composites of Polyamide 11 Filled with Silver Nanowires: Nanocomposites Processing, Mechanical and Electrical Analysis.* Journal of Non-Crystalline Solids, **2013**, 376(0), 199-204.

38. Theng, BKG, *Chapter 7 - Polymer–Clay Nanocomposites*, in *Developments in Clay Science*, Theng BKG, Editor 2012 Elsevier.

39. Ferreira, CI, Dal Castel, C, Oviedo, MS, Mauler, RS, *Isothermal and Non-Isothermal Crystallization Kinetics of Polypropylene/Exfoliated Graphite Nanocomposites.* Thermochimica Acta, **2013**, 553(0), 40-48.

40. Abu-Jdayil, B, *Rheology of Sodium and Calcium Bentonite-Water Dispersions: Effect of Electrolytes and Aging Time.* International Journal of Mineral Processing, **2011**, 98(3-4), 208-213.

41. Kloprogge, JT, Komarneni, S, Amonette, JE, *Synthesis of Smectite Clay Minerals: A Critical Review.* Clays and Clay Minerals, **1999**, 47(5), 529-554.

42. Brown, IWM, Mackenzie, KJD, Meinhold, RH, *The Thermal Reactions of Montmorillonite Studied by High-Resolution Solid-State ^{29}Si and ^{27}Al NMR.* Journal of Materials Science, **1987**, 22(9), 3265-3275.

43. Calderon, JU, Lennox, B, Kamal, MR, *Thermally Stable Phosphonium-Montmorillonite Organoclays.* Applied Clay Science, **2008**, 40(1-4), 90-98.

44. Halim, NA, Ibrahim, ZA, Ahmad, AB, *Intercalation of Water and Guest Molecules within Ca2+-Montmorillonite.* Journal of Thermal Analysis and Calorimetry, **2010**, 102(3), 983-988.

45. Sinha Ray, S, Okamoto, M, *Polymer/Layered Silicate Nanocomposites: A Review from Preparation to Processing.* Progress in Polymer Science, **2003**, 28(11), 1539-1641.

46. Akelah, A, Salahuddin, N, Hiltner, A, Baer, E, Moet, A, *Morphological Hierarchy of Butadieneacrylonitrile/Montmorillonite Nanocomposite.* Nanostructured Materials, **1994**, 4(8), 965-978.

47. Brant, P. *Overview of Drivers and Responses in Polyolefins: Keys to Their Continuing Success*. in *Advances in polyolefins*. 2013. Santa Rosa, USA.

48. Kissel, WJ, Han, JH, Meyer, JA, *Polypropylene: Structure, Properties, Manufacturing Processes, and Applications*, in *Handbook of Polypropylene and Polypropylene Composites*, Karian H, Editor 2003, New York: Marcel Dekker.

49. Chen, B, Evans, JRG, Greenwell, HC, Boulet, P, Coveney, PV, Bowden, AA, Whiting, A, *A Critical Appraisal of Polymer-Clay Nanocomposites.* Chemical Society Reviews, **2008**, 37(3), 568-594.

50. De Rosa, C, Auriemma, F, *Structure and Physical Properties of Syndiotactic Polypropylene: A Highly Crystalline Thermoplastic Elastomer.* Progress in Polymer Science, **2006**, 31(2), 145-237.

51. Karger-Kocsis, J, *Amorphous or Atactic Polypropylene*, in *Polypropylene*, Karger-Kocsis J, Editor 1999 Springer Netherlands.

52. Mckenna, TF, Soares, JBP, *Single Particle Modelling for Olefin Polymerization on Supported Catalysts: A Review and Proposals for Future Developments.* Chemical Engineering Science, **2001**, 56(13), 3931-3949.

53. Yury, K, *Chapter 4 Synthesis, Chemical Composition, and Structure of Transition Metal Components and Cocatalysts in Catalyst Systems for Alkene Polymerization*, in *Studies in Surface Science and Catalysis*, Yury VK, Editor 2007 Elsevier.

54. Cecchin, G, Morini, G, Piemontesi, F, *Ziegler-Natta Catalysts*, in *Kirk-Othmer Encyclopedia of Chemical Technology* 2000 John Wiley & Sons, Inc.

55. Huang, J, Rempel, GL, *Ziegler-Natta Catalysts for Olefin Polymerization: Mechanistic Insights from Metallocene Systems.* Progress in Polymer Science, **1995**, 20(3), 459-526.

56. Chadwick, JC, Heere, JJR, Sudmeijer, O, *Factors Influencing Chain Transfer with Monomer and with Hydrogen in Propene Polymerization Using MgCl2-Supported*

Ziegler-Natta Catalysts. Macromolecular Chemistry and Physics, **2000**, 201(14), 1846-1852.

57. Chu, KJ, Soares, JBP, Penlidis, A, Ihm, SK, *The Influence of the Ti^3 Species on the Microstructure of Ethylene/1-Hexene Copolymers.* Macromolecular Chemistry and Physics, **1999**, 200(6), 1298-1305.

58. Kissin, YV, Mink, RI, Nowlin, TE, Brandolini, AJ, *Kinetics and Mechanism of Ethylene Homopolymerization and Copolymerization Reactions with Heterogeneous Ti-Based Ziegler-Natta Catalysts.* Topics in Catalysis, **1999**, 7(1-4), 69-88.

59. Ogata, N, Kawakage, S, Ogihara, T, *Structure and Thermal/Mechanical Properties of Poly(Ethylene Oxide)-Clay Mineral Blends.* Polymer, **1997**, 38(20), 5115-5118.

60. Billingham, J, Breen, C, Yarwood, J, *Adsorption of Polyamine, Polyacrylic Acid and Polyethylene Glycol on Montmorillonite: An in Situ Study Using ATR-FTIR.* Vibrational Spectroscopy, **1997**, 14(1), 19-34.

61. Qiu, L, Chen, W, Qu, B, *Morphology and Thermal Stabilization Mechanism of LLDPE/MMT and LLDPE/LDH Nanocomposites.* Polymer, **2006**, 47(3), 922-930.

62. Lertwimolnun, W, Vergnes, B, *Influence of Compatibilizer and Processing Conditions on the Dispersion of Nanoclay in a Polypropylene Matrix.* Polymer, **2005**, 46(10), 3462-3471.

63. Pavlidou, S, Papaspyrides, CD, *A Review on Polymer-Layered Silicate Nanocomposites.* Progress in Polymer Science, **2008**, 33(12), 1119-1198.

64. Liu, LM, Qi, ZN, Zhu, XG, *Studies on Nylon 6 Clay Nanocomposites by Melt-Intercalation Process.* Journal of Applied Polymer Science, **1999**, 71(7), 1133-1138.

65. Dennis, HR, Hunter, DL, Chang, D, Kim, S, White, JL, Cho, JW, Paul, DR, *Effect of Melt Processing Conditions on the Extent of Exfoliation in Organoclay-Based Nanocomposites.* Polymer, **2001**, 42(23), 9513-9522.

66. Manias, E, Touny, A, Wu, L, Strawhecker, K, Lu, B, Chung, TC, *Polypropylene/Montmorillonite Nanocomposites. Review of the Synthetic Routes and Materials Properties.* Chemistry of Materials, **2001**, 13(10), 3516-3523.

67. Ton-That, MT, Perrin-Sarazin, F, Cole, KC, Bureau, MN, Denault, J, *Polyolefin Nanocomposites: Formulation and Development.* Polymer Engineering and Science, **2004**, 44(7), 1212-1219.

68. Ristolainen, N, Vainio, U, Paavola, S, Torkkeli, M, Serimaa, R, Seppälä, J, *Polypropylene/Organoclay Nanocomposites Compatibilized with Hydroxyl-Functional Polypropylenes.* Journal of Polymer Science Part B: Polymer Physics, **2005**, 43(14), 1892-1903.

69. Moncada, E, Quijada, R, Lieberwirth, I, Yazdani-Pedram, M, *Use of Pp Grafted with Itaconic Acid as a New Compatibilizer for PP/Clay Nanocomposites.* Macromolecular Chemistry and Physics, **2006**, 207(15), 1376-1386.

70. Nam, BU, Son, Y, *Evaluations of Hema as a Compatibilizer for Polypropylene/Clay Nanocomposites.* Polymer Bulletin, **2010**, 65(8), 837-847.

71. Xu, L, Nakajima, H, Manias, E, Krishnamoorti, R, *Tailored Nanocomposites of Polypropylene with Layered Silicates.* Macromolecules, **2009**, 42(11), 3795-3803.

72. Kotek, J, Kelnar, I, Studenovský, M, Baldrian, J, *Chlorosulfonated Polypropylene: Preparation and Its Application as a Coupling Agent in Polypropylene-Clay Nanocomposites.* Polymer, **2005**, 46(13), 4876-4881.

73. Garcia-Lopez, D, Picazo, O, Merino, JC, Pastor, JM, *Polypropylene-Clay Nanocomposites: Effect of Compatibilizing Agents on Clay Dispersion.* European Polymer Journal, **2003**, 39(5), 945-950.

74. Lapshin, S, Isayev, AI, *Ultrasound-Aided Extrusion Process for Preparation of Polypropylene–Clay Nanocomposites.* Journal of Vinyl and Additive Technology, **2007**, 13(1), 40-45.

75. Kim, DH, Park, JU, Cho, KS, Ahn, KH, Lee, SJ, *A Novel Fabrication Method for Poly(Propylene)/Clay Nanocomposites by Continuous Processing.* Macromolecular Materials and Engineering, **2006**, 291(9), 1127-1135.

76. Liberman, SA, Da Silva, LP, Pelegrini Jr, T, Barbosa, RV, Mauler, RS, *Process for Nanocomposites Preparation*, 2007, BRASKEM , UFRGS. **WO/2007/009200**.

77. Park, S-J, Kim, B-J, Seo, D-I, Rhee, K-Y, Lyu, Y-Y, *Effects of a Silane Treatment on the Mechanical Interfacial Properties of Montmorillonite/Epoxy Nanocomposites.* Materials Science and Engineering: A, **2009**, 526(1–2), 74-78.

78. Azeez, AA, Rhee, KY, Park, SJ, Hui, D, *Epoxy Clay Nanocomposites – Processing, Properties and Applications: A Review.* Composites Part B: Engineering, **2013**, 45(1), 308-320.

79. Tudor, J, Willington, L, Ohare, D, Royan, B, *Intercalation of Catalytically Active Metal Complexes in Phyllosilicates and Their Application as Propene Polymerisation Catalysts.* Chemical Communications, **1996**(17), 2031-2032.

80. Du, K, He, AH, Liu, X, Han, CC, *High-Performance Exfoliated Poly(Propylene)/Clay Nanocomposites by in Situ Polymerization with a Novel Z-N/Clay Compound Catalyst.* Macromolecular Rapid Communications, **2007**, 28(24), 2294-2299.

81. Zeng, QH, Yu, AB, Lu, GQ, *Multiscale Modeling and Simulation of Polymer Nanocomposites.* Progress in Polymer Science, **2008**, 33(2), 191-269.

82. Messersmith, PB, Giannelis, EP, *Synthesis and Characterization of Layered Silicate-Epoxy Nanocomposites.* Chemistry of Materials, **1994**, 6(10), 1719-1725.

83. Lan, T, Pinnavaia, TJ, *Clay-Reinforced Epoxy Nanocomposites.* Chemistry of Materials, **1994**, 6(12), 2216-2219.

84. Svoboda, P, Zeng, C, Wang, H, Lee, LJ, Tomasko, DL, *Morphology and Mechanical Properties of Polypropylene/Organoclay Nanocomposites.* Journal of Applied Polymer Science, **2002**, 85(7), 1562-1570.

85. Luo, JJ, Daniel, IM, *Characterization and Modeling of Mechanical Behavior of Polymer/Clay Nanocomposites.* Composites Science and Technology, **2003**, 63(11), 1607-1616.

86. Luo, J-J, Daniel, IM, *Characterization and Modeling of Mechanical Behavior of Polymer/Clay Nanocomposites.* Composites Science and Technology, **2003**, 63(11), 1607-1616.

87. Sheng, N, Boyce, MC, Parks, DM, Rutledge, GC, Abes, JI, Cohen, RE, *Multiscale Micromechanical Modeling of Polymer/Clay Nanocomposites and the Effective Clay Particle.* Polymer, **2004**, 45(2), 487-506.

88. Kojima, Y, Usuki, A, Kawasumi, M, Okada, A, Kurauchi, T, Kamigaito, O, *One-Pot Synthesis of Nylon 6–Clay Hybrid.* Journal of Polymer Science Part A: Polymer Chemistry, **1993**, 31(7), 1755-1758.

89. Nam, PH, Maiti, P, Okamoto, M, Kotaka, T, Nakayama, T, Takada, M, Ohshima, M, Usuki, A, Hasegawa, N, Okamoto, H, *Foam Processing and Cellular Structure of Polypropylene/Clay Nanocomposites.* Polymer Engineering & Science, **2002**, 42(9), 1907-1918.

90. Yano, K, Usuki, A, Okada, A, Kurauchi, T, Kamigaito, O, *Synthesis and Properties of Polyimide Clay Hybrid.* Journal of Polymer Science Part A-Polymer Chemistry, **1993**, 31(10), 2493-2498.

91. Ray, SS, Yamada, K, Okamoto, M, Ogami, A, Ueda, K, *New Polylactide/Layered Silicate Nanocomposites. 3. High-Performance Biodegradable Materials.* Chemistry of Materials, **2003**, 15(7), 1456-1465.

92. Nielsen, LE, *Models for the Permeability of Filled Polymer Systems.* Journal of Macromolecular Science, Part A, **1967**, 1(5), 929 - 942.

93. Bharadwaj, RK, *Modeling the Barrier Properties of Polymer-Layered Silicate Nanocomposites.* Macromolecules, **2001**, 34(26), 9189-9192.

94. Lakshmi, AS, Narmadha, B, Redd, BSR, *Enhanced Thermal Stability and Structural Characteristics of Different MMT-Clay/Epoxy-Nanocomposite Materials.* Polymer Degradation and Stability, **2008**, 93(1), 201-213.

95. Lai, MC, Chang, KC, Huang, WC, Hsu, SC, Yeh, JM, *Effect of Swelling Agent on the Physical Properties of Pet-Clay Nanocomposite Materials Prepared from Melt Intercalation Approach.* Journal of Physics and Chemistry of Solids, **2008**, 69(5-6), 1371-1374.

96. Carrasco, F, Pages, P, *Thermal Degradation and Stability of Epoxy Nanocomposites: Influence of Montmorillonite Content and Cure Temperature.* Polymer Degradation and Stability, **2008**, 93(5), 1000-1007.

97. Kim, S, Wilkie, CA, *Transparent and Flame Retardant Pmma Nanocomposites.* Polymers for Advanced Technologies, **2008**, 19(6), 496-506.

98. Sanli, D, Bozbag, SE, Erkey, C, *Synthesis of Nanostructured Materials Using Supercritical Co2: Part I. Physical Transformations.* Journal of Materials Science, **2012**, 47(7), 2995-3025.

99. E, S, Kw, Q, D, G, *Dense Gases for Extraction and Refining*1988, New York: Springer-Verlag.

100. Ambrose, D, Tsonopoulos, C, *Vapor-Liquid Critical Properties of Elements and Compounds .2. Normal-Alkanes.* Journal of Chemical and Engineering Data, **1995**, 40(3), 531-546.

101. Tsonopoulos, C, Ambrose, D, *Vapor-Liquid Critical Properties of Elements and Compounds .3. Aromatic-Hydrocarbons.* Journal of Chemical and Engineering Data, **1995**, 40(3), 547-558.

102. Air Liquide, Propylene Technical Specificaiton *www.Airliquide.Com/*. Accessed in Jan 16, 2013].

103. Lemmon, EW, Goodwin, ARH, *Critical Properties and Vapor Pressure Equation for Alkanes CH_{2n+2}: Normal Alkanes with N⩽36 and Isomers for N=4 through N=9.* Journal of Physical and Chemical Reference Data, **2000**, 29(1), 1-39.

104. Ma, J, Bilotti, E, Peijs, T, Darr, JA, *Preparation of Polypropylene/Sepiolite Nanocomposites Using Supercritical CO_2 Assisted Mixing.* European Polymer Journal, **2007**, 43(12), 4931-4939.

105. Hwang, TY, Lee, SM, Ahn, Y, Lee, JW, *Development of Polypropylene-Clay Nanocomposite with Supercritical CO_2 Assisted Twin Screw Extrusion.* Korea-Australia Rheology Journal, **2008**, 20(4), 235-243.

106. Yang, K, Ozisik, R, *Effects of Processing Parameters on the Preparation of Nylon 6 Nanocomposites.* Polymer, **2006**, 47(8), 2849-2855.

107. Horsch, S, Serhatkulu, G, Gulari, E, Kannan, RM, *Supercritical CO_2 Dispersion of Nano-Clays and Clay/Polymer Nanocomposites.* Polymer, **2006**, 47(21), 7485-7496.

108. Kissin, Y, *Chapter 6 Active Centers in Transition Metal Catalysts and Mechanisms of Polymerization Reactions*, in *Studies in Surface Science and Catalysis*, Yury VK, Editor 2007Elsevier.

109. Liberman, SA, Pozzer, DA, Mota, FF, Martins, JO, Silva Neto, ML, *A Process for Polymerization in the Presence of Nanoparticles of a Mineral Filler for the Attainment of Polymer Nanocomposites, and a Polymer Nanocomposite*, 2009. **WO/2009/052595**

110. Kissin, Y, *Chapter 5 Kinetics of Alkene Polymerization Reactions with Transition Metal Catalysts*, in *Studies in Surface Science and Catalysis*, Yury VK, Editor 2007 Elsevier.

111. Reichardt, C, Welton, T, in *Solvents and Solvent Effects in Organic Chemistry*2010Wiley-VCH Verlag GmbH & Co. KGaA.

112. Bu, HS, Cheng, SZD, Wunderlich, B, *Addendum to the Thermal-Properties of Polypropylene.* Makromolekulare Chemie-Rapid Communications, **1988**, 9(2), 75-77.

113. Foster, MD, *Geochemical Studies of Clay Minerals: (Ii)–Relation between Ionic Substitution and Swelling in Montmorillonite.* American Mineralogist, **1953**, 38(11), 994-1006.

114. Maneshi, A, Soares, JBP, Simon, LC, *Polyethylene/Clay Nanocomposites Made with Metallocenes Supported on Different Organoclays.* Macromolecular Chemistry and Physics, **2011**, 212(3), 216-228.

115. Maneshi, A, Soares, J, Simon, L, *Polyolefin–Clay Nanocomposites by in-Situ Polymerization*, in *In-Situ Synthesis of Polymer Nanocomposites* 2011 Wiley-VCH Verlag GmbH & Co. KGaA.

116. Lee, D-H, Kim, H-S, Yoon, K-B, Min, KE, Seo, KH, Noh, SK, *Polyethylene/Mmt Nanocomposites Prepared by in Situ Polymerization Using Supported Catalyst Systems.* Science and Technology of Advanced Materials, **2005**, 6(5), 457-462.

117. Burfield, DR, Loi, PST, *The Use of Infrared Spectroscopy for Determination of Polypropylene Stereoregularity.* Journal of Applied Polymer Science, **1988**, 36(2), 279-293.

118. Järvelä, P, Shucai, L, Järvelä, P, *Dynamic Mechanical Properties and Morphology of Polypropylene/Maleated Polypropylene Blends.* Journal of Applied Polymer Science, **1996**, 62(5), 813-826.

119. Ribour, D, Bollack-Benoit, V, Monteil, V, Spitz, R, *Exploring Pathways to Reduce the Distribution of Active Sites in the Ziegler–Natta Polymerization of Propylene.* Journal of Polymer Science Part A: Polymer Chemistry, **2007**, 45(17), 3941-3948.

120. Naik, SD, Ray, WH, *Particle Morphology for Polyolefins Synthesized with Supported Metallocene Catalysts.* Journal of Applied Polymer Science, **2001**, 79(14), 2565-2579.

Appendix A. Pressure vessel and fixtures from Parker Autoclave Engineers.

Parts used to assembly the pressure vessel.

Description	Quantity	Item SKU
High pressure	01	KD10.3SS11
Tubing Nipple	08	CN6603
Cross	01	CX6666
Tee	01	CT6660
Safety head	01	CS6600-3/16F
Rupture disc	06	P-7032
Pressure gauge	01	P-0482-GC
Valve	02	30VM4071-TG
Adapter	01	6M64B2
Adapter	01	15M62B1
Thermocouple	01	MTCSK06024
Elbow	01	CL6660
Nut	01	SMNIO
Sleeve	01	SSLIO
Adapter	01	15M64B8

Double Ended Series KD

MODEL NUMBER	NOMINAL CAPACITY	Dimensions: Inches (mm)			
		I. DIA	O. DIA	I.L.	OAL
KD10.3SS11 DOUBLE ENDED	103 ml	1.00" (25.4)	2.13" (54.1)	8.00" (203.2)	13.00" (330.2)
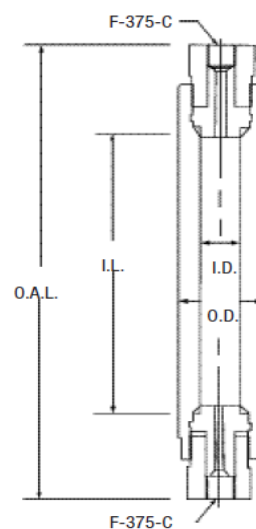
Appendix B. Polymerization reactor and pressure vessel for supercritical propylene.
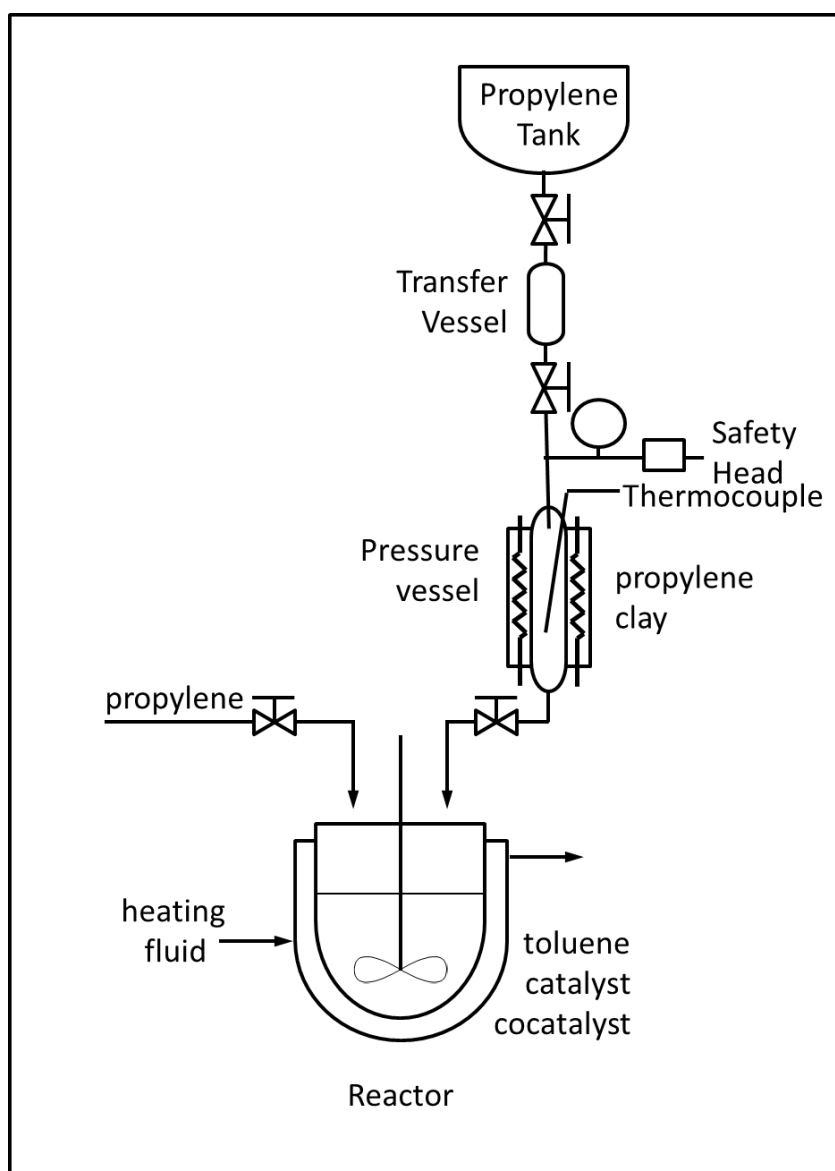
Appendix C. Selected pictures showing clay swelling test results.

All pictures present the clays in the following order from left to right: Na+, 10A, 15A, 20A, 30B, 93A, I.44P and I.31PS. The solvent, mixing condition, and settling time are described in the figure caption.
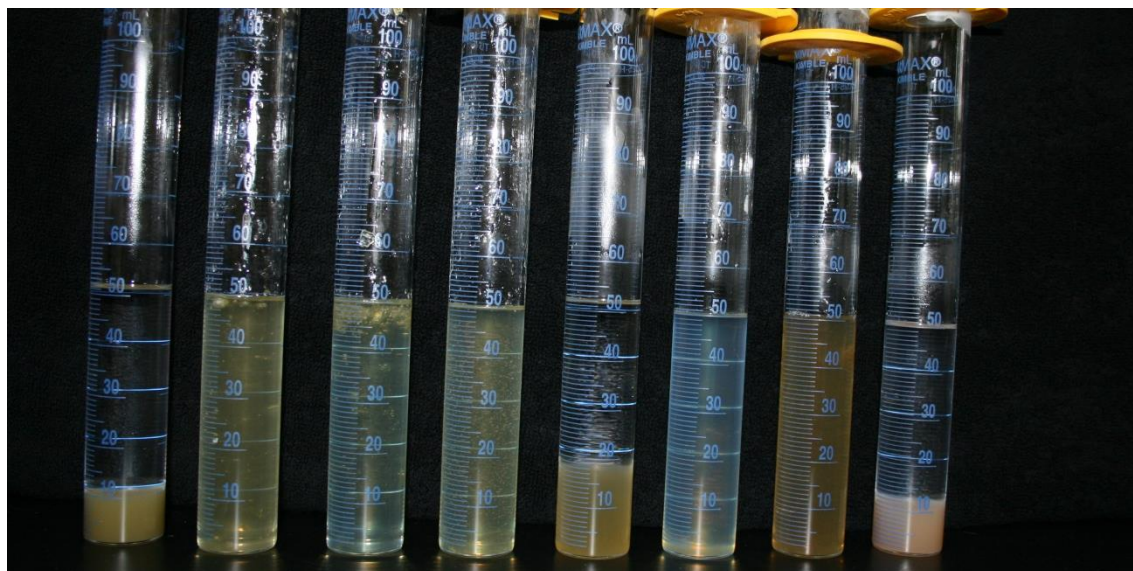

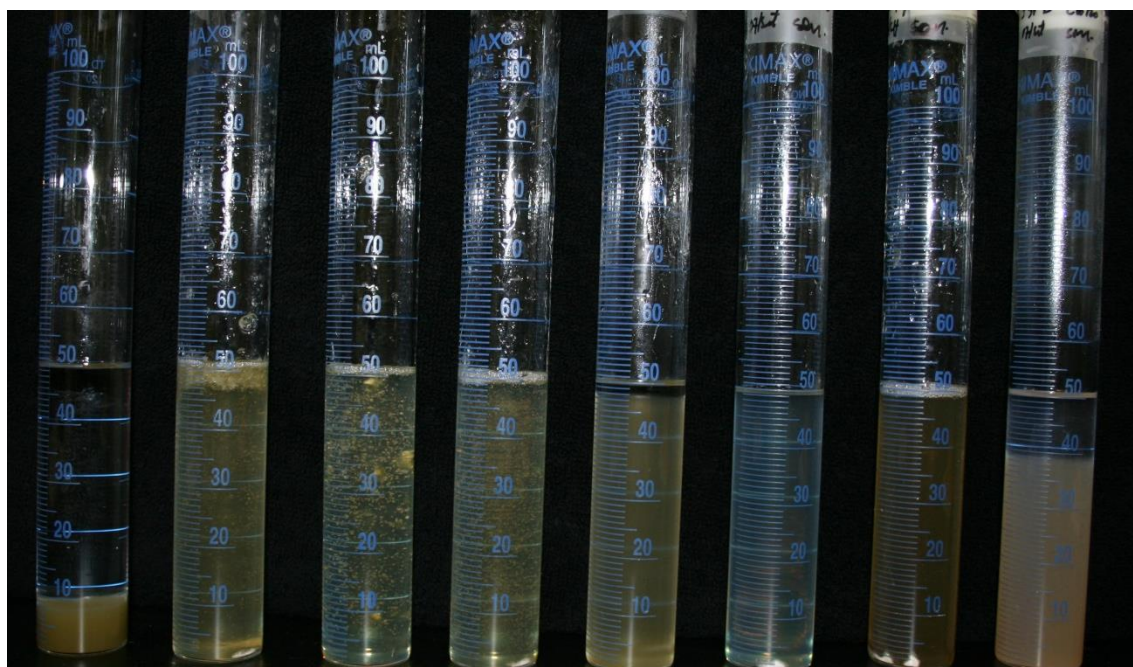**Figure 33**. Chlorobenzene, manual mixing, zero day.

Figure 34. Chlorobenzene, ultrasonic bath, zero day.

Figure 35. Chlorobenzene, ultrasonic bath, 28 days.

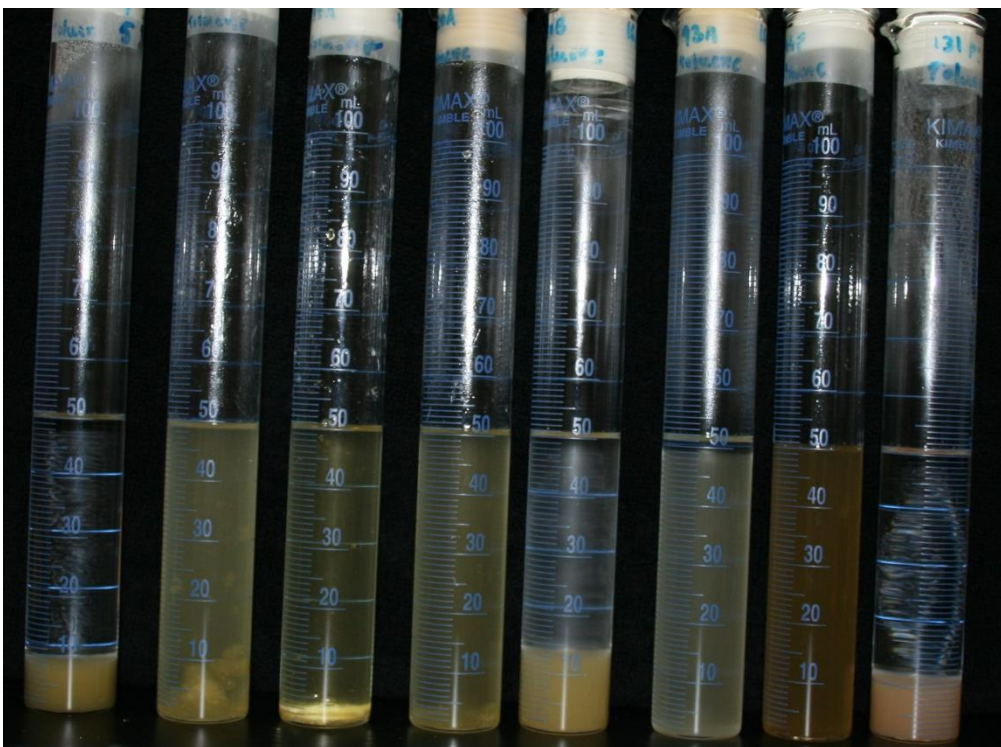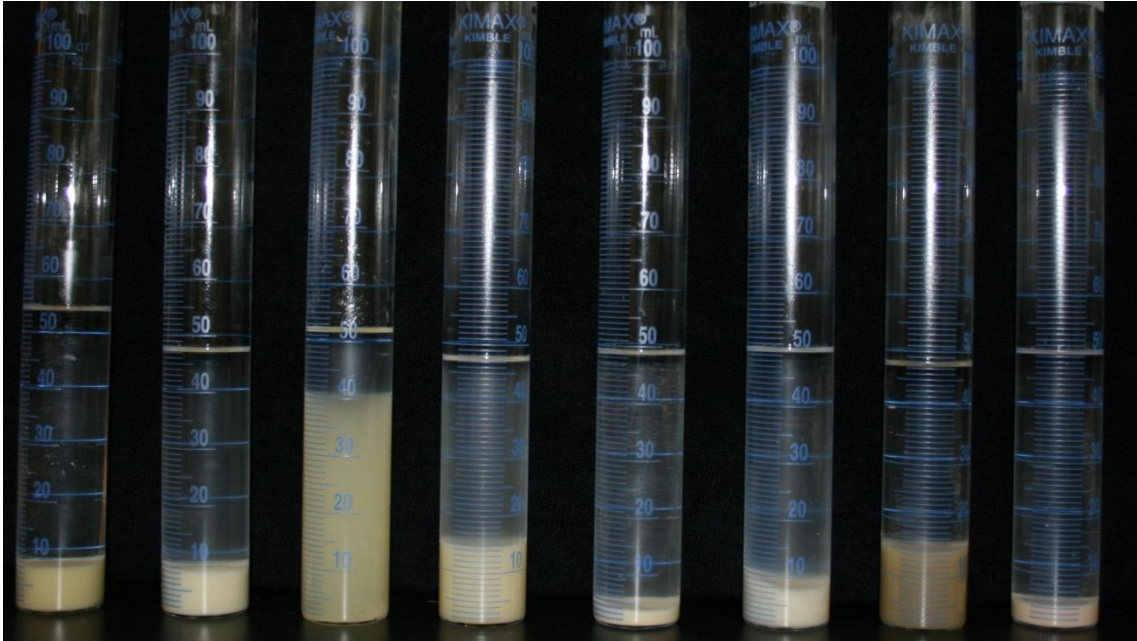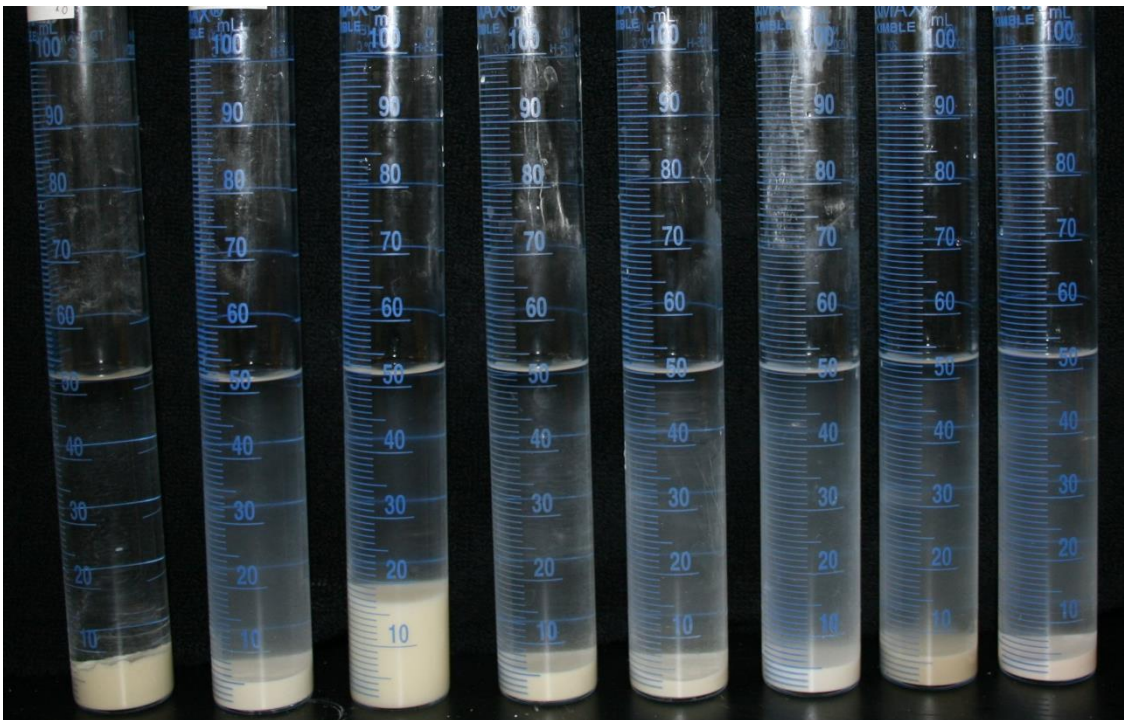**Figure 36.** Toluene, manual mixing, zero day.

Figure 37. Cyclohexane, manual mixing, one day.

Figure 38. Hexane, manual mixing, 1 day.